

NASA Technical Paper 1675

Some Design Considerations for Solar-Powered Aircraft

William H. Phillips

JUNE 1980

NASA

NASA Technical Paper 1675

Some Design Considerations for Solar-Powered Aircraft

William H. Phillips
Langley Research Center
Hampton, Virginia



National Aeronautics
and Space Administration

**Scientific and Technical
Information Office**

1980

CONTENTS

SUMMARY	1
INTRODUCTION	1
SYMBOLS	2
ANALYSIS	5
Climb Efficiency	5
The Term $1 - \frac{D}{T}$	7
Propeller Efficiency	7
Calculation of Rate of Climb	9
Calculation of Power for Level Flight or of Absolute Ceiling	11
Calculation of Time to Climb	11
Calculation of Time to Descend	11
EXAMPLES OF PERFORMANCE CAPABILITIES OF	
SOLAR-POWERED AIRCRAFT	14
Analytical Approach	14
Flight at Constant Altitude	14
Solar energy received	15
Energy required	15
Aircraft parameters	16
Calculation of length of night	17
Presentation of results	17
Region of feasible operation	18
Flight With Varying Altitude	19
Considerations of climb efficiency	19
Use of constant lift coefficient	20
Flight profile without energy storage devices	20
Presentation of results	21
Flight profile with energy storage devices	21
Parameters assumed	22
Presentation of results	23
Regions of feasible operation	23
DISCUSSION OF RESULTS	24
Effect of Changes in System Parameters	24
Effect of Mode of Operation	24
Design Considerations	25
Wing loading	25

Solar-cell and battery technology	26
Motor technology	26
Aerodynamics	26
Practical Aspects of Design of a Solar-Powered Aircraft	28
Size, structural weight, and loading conditions	28
Solar-cell arrangement	28
CONCLUDING REMARKS	30
APPENDIX – ANALYSIS OF LIFT AND INDUCED DRAG OF A CRUCIFORM WING AT VARIOUS ROLL ANGLES	31
REFERENCES	33
TABLE	34
FIGURES	35

SUMMARY

Developments in the areas of structures, solar cells, and energy storage devices have introduced the possibility of an aircraft which will stay aloft overnight by using energy from the Sun's rays stored during the daytime. Such an aircraft, even if it is unmanned and carries a small payload, may have useful applications such as atmospheric monitoring, communications, and reconnaissance.

This report presents some analytical developments which may be useful in calculating the performance characteristics of such a vehicle and gives the results of a study to determine its operational characteristics and limitations. A discussion of practical design considerations is also presented.

The wing loading of a solar-powered aircraft should be as low as possible, limited only by the need for the flight speed to exceed the wind speed at the operating altitude. Wind considerations set the minimum wing loading at about 15 N/m^2 and the minimum operating altitude at about 20 km. Presently available solar cells are adequate for operation of such a vehicle, but existing rechargeable batteries are too heavy. A flight plan consisting of climbing in the day to store energy and gliding at night is not feasible because the altitude lost during the night is excessive. Projected developments of fuel-cell energy storage systems appear to make the solar-powered aircraft feasible.

INTRODUCTION

The possibility of powering an aircraft by solar energy has been considered by a number of investigators. A study of a manned solar-powered airplane, similar in design to a soaring glider, is given in reference 1. The report shows that such an aircraft could be kept aloft by energy from photovoltaic solar cells during daylight hours. A number of unmanned, solar-powered aircraft have been successfully flown, as, for example, those described in references 2 and 3. Some manned aircraft have flown on power supplied by a battery charged by solar energy (ref. 4). None of these aircraft, however, had the capability of flying during the day and storing enough solar energy to remain aloft during the night.

With the development of improved aerodynamic configurations and structural design, particularly as embodied in the man-powered airplanes of Paul MacCready (refs. 5 and 6), the possibility has been recognized that a solar-powered aircraft might be built which

would stay aloft overnight. This goal might be accomplished by using energy stored in batteries during the daytime, by climbing during the day and gliding during the night, or by some combination of these methods. This capability leads to the ability of such an aircraft to remain aloft indefinitely. The ability to maintain a vehicle in flight for extended periods, even if it is unmanned and carries a very small payload, offers useful applications such as atmospheric monitoring, communications, and reconnaissance. A review of environmental applications of such an aircraft and some considerations of its design are given in reference 7.

The purpose of this report is to present some analytical developments which may be useful in calculating the performance characteristics of such a vehicle and to give the results of a simplified analysis to establish guidelines for the aerodynamic and operational characteristics required. The critical technologies which limit the performance are identified, and improvements required to meet desired performance goals are discussed.

The performance analysis methods described include calculation of rate of climb and time to climb through a variable-density atmosphere, determination of power for level flight and of absolute ceiling, and calculation of time to descend through a variable-density atmosphere. No approximations are made which limit the application of the results to small climb angles. The reduction in propeller efficiency with increased climb angle, which results from increased thrust coefficient and hence increased energy loss in the slipstream, is taken into account.

The analysis considers flight plans involving flight at constant altitude and flight consisting of climbing in the day to store energy and gliding in the night, both with and without additional energy storage devices. The studies are based on assumed parameters for the performance of components of the propulsion system, but the effects of changes in these parameters may be readily determined. Regions of feasible operation for the various modes of operation are presented in terms of wing loading and altitude.

Finally, some discussion is included of the practical design problems of aerodynamic efficiency, structural design, and propulsion-system arrangement.

SYMBOLS

- | | |
|---|--|
| A | effective aspect ratio |
| a | ratio of incremental velocity in slipstream to airspeed |
| C | fractional reduction in propeller efficiency below Froude efficiency |

C_D	drag coefficient, D/qS
$C_{D,0}$	profile drag coefficient
C_L	lift coefficient, L/qS
$C_{L,max}$	maximum lift coefficient
C_T	thrust coefficient, $\frac{T}{\frac{\pi}{8} \rho V^2 d^2}$
c	ratio of square of propeller diameter to wing area, d^2/S
D	drag
d	propeller diameter
E	energy
e	base of natural logarithms
F	latitude angle
g_0	acceleration of gravity at sea level, 9.80665 m/sec^2
h	altitude above sea level or, in equations (30) and (35), above reference altitude
h_{base}	minimum altitude used in a constant-altitude segment of flight
h_{max}	maximum altitude used in a constant-altitude segment of flight
K	factor related to rate of descent (eq. (28))
K_1, K_2, K_3, K_4	constants defined in equations (32) and (37)
L	lift
L'_M	gradient of temperature with geopotential altitude

M	Mach number
M_o	molecular weight of air at sea level, 28.9644
P	power
P_b	pressure at reference altitude
p	ratio of thrust to drag, $\frac{\tan \gamma + (C_D/C_L)}{C_D/C_L}$
q	dynamic pressure, $\rho V^2/2$
R^*	universal gas constant, 8.31432 J/K-mol
S	wing area, or other area denoted by subscript
T	thrust
$T_{M,b}$	molecular-scale temperature at base altitude, K
t	time
t_{day}	time solar-powered aircraft spends in daylight during each 24-hr period, hr
t_{night}	time solar-powered aircraft spends in darkness during each 24-hr period, hr
V	true airspeed
W	weight
W_T	total weight
γ	flight-path angle
δ	component of tilt of Earth's axis from normal to Sun-Earth line
η	propeller efficiency

η_c	climb efficiency
η_F	Froude efficiency
ν	viscosity
ρ	air density
τ	time after fall equinox, days

Subscripts:

b	batteries
c	solar cells
m	motor

A subscript notation is used to make the symbols for the parameters of the system self-explanatory. Thus, for example,

$\left(\frac{P}{W}\right)_c$ ratio of power output to weight of solar cells

$\left(\frac{W}{S}\right)_c$ ratio of weight to area of solar cells

$\left(\frac{E}{W}\right)_b$ ratio of energy output to weight of batteries

A dot over a symbol denotes differentiation with respect to time.

ANALYSIS

Climb Efficiency

In the operation of solar-powered aircraft, excess energy which is available during the daylight hours may be stored either as chemical energy by charging batteries or as potential energy by climbing. Consider the method of storing energy by climbing. A fundamental problem is to determine the conditions under which the aircraft should be

flown so that the ratio of potential energy stored to energy produced by the motor is a maximum.

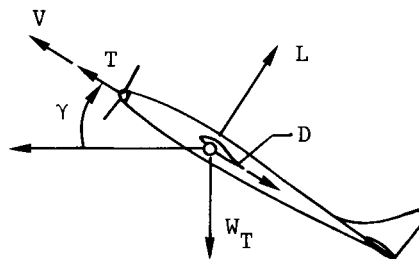
The rate at which potential energy is stored is the rate of climb \dot{h} multiplied by the total weight W_T . If all the thrust horsepower available from the motor went into producing climb, this rate of change of potential energy would equal the motor power P_m multiplied by propeller efficiency η . In practice, not all the thrust horsepower is used for climb, as some is used to overcome aerodynamic drag. The fraction so used is D/T , where D is the drag of the vehicle and T is the thrust. The equation for the rate of change of potential energy is therefore

$$\dot{h}W_T = P_m \eta \left(1 - \frac{D}{T}\right)$$

In other words, the fraction of the work done by the motor converted to potential energy is

$$\eta_c = \frac{\dot{h}W_T}{P_m} = \eta \left(1 - \frac{D}{T}\right) \quad (1)$$

This equation gives the mechanical efficiency of converting the work done by the motor to potential energy. This quantity will be referred to hereinafter as the "climb efficiency." In level flight, $D = T$ so that no change in potential energy occurs and the climb efficiency is zero. The terms in equation (1) are now expressed in terms of the lift coefficient C_L , the flight-path angle γ , and other aerodynamic parameters of the vehicle. Consider the accompanying diagram of the forces acting on an airplane in a steady climb. The following relations may be obtained:



$$T - D = W_T \sin \gamma \quad (2)$$

$$L = W_T \cos \gamma \quad (3)$$

Dividing equation (2) by equation (3) gives

$$\frac{T - D}{L} = \tan \gamma \quad (4)$$

The Term $1 - \frac{D}{T}$

Substituting the value of T from equation (4) into the expression $1 - \frac{D}{T}$ gives

$$1 - \frac{D}{T} = 1 - \frac{D}{L \tan \gamma + D} = 1 - \frac{D/L}{\tan \gamma + \frac{D}{L}} = 1 - \frac{C_D/C_L}{\tan \gamma + \frac{C_D}{C_L}} \quad (5)$$

The value of C_D is assumed to be given as a function of C_L by the relation

$$C_D = C_{D,o} + \frac{C_L^2}{\pi A} \quad (6)$$

Thus, the term $1 - \frac{D}{T}$ may be expressed in terms of C_L and γ .

Propeller Efficiency

For purposes of this analysis, an approximate calculation of propeller efficiency is made. The value used is simply the so-called Froude efficiency (ref. 8), which is reduced by a constant to account for the losses due to profile drag of the blades and non-uniformity of flow in the slipstream. The Froude efficiency accounts for the energy lost in creating axial momentum in the slipstream. This method of calculating efficiency is reasonably accurate for propellers operating near the value of advance ratio for peak efficiency. The use of this method implies that the propeller is adjusted to match the flight condition through use of variable pitch or variable gearing. In textbooks on propeller theory, such as reference 8, the Froude efficiency is shown to be

$$\eta_F = \frac{1}{1 + \frac{a}{2}} \quad (7)$$

where a is the ratio of incremental velocity in the slipstream to the flight speed.

This efficiency is now related to the propeller thrust. Define a thrust coefficient based on the propeller disk area as

$$C_T = \frac{T}{\frac{\rho}{2} V^2 \frac{\pi}{4} d^2} = \frac{T}{\frac{\pi}{8} \rho V^2 d^2} \quad (8)$$

By equating the thrust to the rate of change of momentum through the propeller disk, it may be shown that

$$C_T = 2a \left(1 + \frac{a}{2} \right) \quad (9)$$

The thrust coefficient may therefore be expressed in terms of the Froude efficiency

$$C_T = \frac{4}{\eta_F} \left(\frac{1}{\eta_F} - 1 \right) = 4 \left(\frac{1 - \eta_F}{\eta_F^2} \right) \quad (10)$$

Using the definition of thrust coefficient and the value of T/D from equation (5)

$$C_T = \frac{C_D \frac{\rho}{2} V^2 S T}{\frac{\pi}{8} \rho V^2 d^2 D} = \frac{4C_D}{\pi \frac{d^2}{S}} \left(\frac{\tan \gamma + \frac{C_D}{C_L}}{C_D/C_L} \right) \quad (11)$$

For simplicity, let

$$\left. \begin{aligned} c &= \frac{d^2}{S} \\ p &= \frac{\tan \gamma + \frac{C_D}{C_L}}{C_D/C_L} \end{aligned} \right\} \quad (12)$$

where p is the ratio of thrust to drag. Then

$$C_T = \frac{4C_D p}{\pi c} = 4 \left(\frac{1 - \eta_F}{\eta_F^2} \right) \quad (13)$$

This relation leads to a quadratic equation for η_F , which may be solved to give η_F in terms of quantities depending on C_L and γ and the additional quantities C_D and c .

$$\eta_F = \frac{-1 + \sqrt{1 + \frac{4pC_D}{\pi c}}}{2 \frac{pC_D}{\pi c}} \quad (14)$$

The overall propeller efficiency is then assumed to be

$$\eta = \eta_F - C = \frac{-1 + \sqrt{1 + \frac{4pC_D}{\pi c}}}{2 \frac{pC_D}{\pi c}} - C \quad (15)$$

where the value of C is taken as 0.1 in the subsequent calculations.

By substituting equations (5) and (14) in equation (1), the efficiency of storing energy in a climb may be expressed in terms of the parameters C_D , C_L , γ , c , and C .

Calculation of Rate of Climb

Calculation of the rate of climb using equation (1) requires, in addition to the climb efficiency factor already described, the ratio of motor power to total weight P_m/W_T . Even if this quantity is given, however, a pair of values of flight-path angle γ and lift coefficient C_L must be determined to be compatible with the available power-weight ratio. In order to determine this relationship, the equation relating engine power to thrust horsepower is utilized

$$P_m \eta = TV \quad (16)$$

or

$$P_m = \frac{TV}{\eta} = \frac{pDV}{\eta} \quad (17)$$

By definition,

$$D = C_D \frac{\rho}{2} V^2 S \quad (18)$$

and, from equation (3),

$$L = C_L \frac{\rho}{2} V^2 S = W_T \cos \gamma \quad (19)$$

Substituting equation (18) in equation (17),

$$P_m = \frac{\rho C_D \frac{\rho}{2} V^3 S}{\eta} \quad (20)$$

Solving equation (19) for V and substituting this value in equation (20) gives

$$\frac{P_m}{W_T} = \frac{\rho C_D (\cos \gamma)^{3/2} \left(\frac{W_T}{S}\right)^{1/2}}{\eta C_L^{3/2} \left(\frac{\rho}{2}\right)^{1/2}} \quad (21)$$

Substituting the value of η from equation (15) in equation (21) yields an equation in which the variables are P_m/W_T , C_L , γ , ρ , W_T/S , and c . Any one of these quantities may be determined if the others are given. Solution for one of the variables in terms of the others, however, requires solution of an equation of fourth degree or higher. An iterative solution is usually the most convenient procedure.

One problem of interest is to determine the lift coefficient for steady climb, given the other variables. This problem may be solved iteratively by selecting an initial value of lift coefficient (zero will do), calculating propeller efficiency from equation (15), then substituting this value in equation (21) and solving for the lift coefficient. This new value of lift coefficient is used to calculate a new value of propeller efficiency, and the process is repeated until the difference between two successive values of lift coefficient is less than some specified small value. After the lift coefficient has been calculated, the air-speed may be determined from equation (19) and the rate of climb may be found from the relation

$$\dot{h} = V \sin \gamma \quad (22)$$

or from equation (1).

An application of this method is to determine the maximum rate of climb at any altitude. Successively higher values of γ are assumed and the corresponding rates of climb are calculated by the foregoing method until either the maximum value is reached or the specified maximum lift coefficient is reached.

A second problem is to calculate the climb angle γ and hence the rate of climb, given the lift coefficient and the other variables. Equation (21) is not in the most desirable form for this procedure because $\cos \gamma$ does not vary greatly from one at small values of γ . A more efficient procedure is to solve equation (21) for ρ , then to substitute this

value into equations (12) which may be solved for $\tan \gamma$. The result is

$$\tan \gamma = \frac{C_D}{C_L} \left[\frac{\frac{P_m}{W_T} \eta C_L^{3/2} \left(\frac{\rho}{2}\right)^{1/2}}{C_D (\cos \gamma)^{3/2} \left(\frac{W_T}{S}\right)^{1/2}} - 1 \right] \quad (23)$$

Initially, values are assumed for η and $\cos \gamma$ (a value of one may be assumed for each), allowing the determination of $\tan \gamma$ and γ from equation (23). This value is then used to calculate η from equation (15) and to provide a better approximation to $\cos \gamma$ in the next iteration. The process is repeated until the error in γ is less than some specified small value. The value of rate of climb may then be calculated from equation (1) or (22).

Calculation of Power for Level Flight or of Absolute Ceiling

The power for level flight or the air density at the absolute ceiling may readily be calculated from equations (21) and (15) by setting $\gamma = 0$. In this case, $p = 1$. The equations may be solved directly if C_L is given. Otherwise, the iterative procedure described previously to determine C_L may be used. In many cases, the optimum value of C_L based on a parabolic drag polar will be beyond a reasonable value of maximum lift coefficient. The assumption of $C_L = C_{L,max}$ is used in this case.

Calculation of Time to Climb

The pressure, temperature, and density at any altitude in the standard atmosphere may be determined from equations and tables given in reference 9. From the air density and other aircraft parameters specified previously, the rate of climb at a series of values of altitude is determined. Time to climb is then obtained from the equation

$$t = \int \frac{dh}{\dot{h}} \quad (24)$$

A trapezoidal integration is used herein to evaluate the time to climb numerically.

Calculation of Time to Descend

Rate of descent in a power-off glide is determined by equating the power exerted by gravity to the power used in overcoming aerodynamic drag

$$W_T \dot{h} = DV \quad (25)$$

or

$$\dot{h} = \frac{DV}{W_T} = \frac{C_D \frac{\rho}{2} V^3 S}{W_T} \quad (26)$$

From equation (19),

$$V^3 = \left(\frac{W_T \cos \gamma}{C_L \frac{\rho}{2} S} \right)^{3/2} \quad (27)$$

Substituting equation (27) in equation (26),

$$\dot{h} = \frac{C_D}{C_L^{3/2}} \left(\frac{W_T}{S} \right)^{1/2} \frac{(\cos \gamma)^{3/2}}{\left(\frac{\rho}{2} \right)^{1/2}} = \frac{K}{\left(\frac{\rho}{2} \right)^{1/2}} \quad (28)$$

where

$$K = \frac{\left(\frac{W_T}{S} \right)^{1/2} (\cos \gamma)^{3/2}}{C_L^{3/2} / C_D}$$

Normally, the glide angle is 3° or less for L/D greater than 20, and the value of $\cos \gamma$ is close to 1.0. The time to descend between altitudes h_1 and h_2 is then obtained by substituting equation (28) into equation (24)

$$t = \frac{1}{K} \int_{h_1}^{h_2} \left(\frac{\rho}{2} \right)^{1/2} dh \quad (29)$$

In the NASA standard atmosphere (ref. 9), the altitude is divided into segments in which the temperature is either constant or varying linearly with altitude. In each of these segments, the density is expressed by equations for which equation (29) may be integrated in closed form. In the constant-temperature segments, using the notation of reference 9,

$$\rho = \frac{P_b M_o}{R^* T_{M,b}} e^{\left(\frac{-g_o M_o h}{R^* T_{M,b}} \right)} \quad (30)$$

or

$$\left(\frac{\rho}{2} \right)^{1/2} = \sqrt{\frac{P_b M_o}{2R^* T_{M,b}}} e^{\left(\frac{-g_o M_o h}{2R^* T_{M,b}} \right)} \quad (31)$$

$$\left(\frac{\rho}{2} \right)^{1/2} = K_1 e^{-K_2 h} \quad (32)$$

Substituting this value in equation (29),

$$t = \frac{K_1}{K} \int_{h_1}^{h_2} e^{-K_2 h} dh \quad (33)$$

Integrating yields

$$t = -\frac{K_1}{KK_2} \left(e^{-K_2 h_2} - e^{-K_2 h_1} \right) \quad (34)$$

In the segments in which temperature varies linearly with altitude,

$$\rho = \frac{P_b M_o \left(\frac{T_{M,b}}{T_{M,b} + L'_M h} \right)^{\frac{g_o M_o}{R^* L'_M}}}{R^* (T_{M,b} + L'_M h)} \quad (35)$$

$$\left(\frac{\rho}{2} \right)^{1/2} = \sqrt{\frac{P_b M_o}{2R^*}} \frac{(T_{M,b})^{\frac{g_o M_o}{2R^* L'_M}}}{(T_{M,b} + L'_M h) \left(1 + \frac{g_o M_o}{R^* L'_M} \right)^{1/2}} \quad (36)$$

$$\left(\frac{\rho}{2}\right)^{1/2} = K_3 \frac{(T_{M,b})^{K_4/2}}{(T_{M,b} + L'_M h)^{(1+K_4)/2}} \quad (37)$$

Substituting this value in equation (29),

$$t = \frac{K_3}{K} (T_{M,b})^{K_4/2} \int_{h_1}^{h_2} (T_{M,b} + L'_M h)^{-(1+K_4)/2} dh \quad (38)$$

Integrating yields

$$t = \frac{K_3}{K} (T_{M,b})^{K_4/2} \left[\frac{(T_{M,b} + L'_M h_2)^{(1-K_4)/2} - (T_{M,b} + L'_M h_1)^{(1-K_4)/2}}{L'_M \left(\frac{1-K_4}{2}\right)} \right] \quad (39)$$

EXAMPLES OF PERFORMANCE CAPABILITIES OF SOLAR-POWERED AIRCRAFT

Analytical Approach

The method of analysis used herein is to calculate the energy and weight requirements for a given type of flight operation at a series of values of wing loading and altitude. For any given values of the efficiencies and specific weights of the major components such as solar cells, batteries, and motor, the feasible regions of operation in terms of wing loading and altitude may be determined. The effect of improvements in these technologies in increasing the range of feasible operation may also be studied.

Flight at Constant Altitude

The simplest flight plan for a solar-powered aircraft is to maintain constant altitude. During the day, the photovoltaic solar cells or other solar energy conversion devices supply energy both to maintain level flight and to charge the batteries or other energy storage devices. During the night, the aircraft maintains level flight on battery power alone.

Solar energy received. - The amount of solar energy received by the aircraft depends on the length of day, the attenuation of the solar energy by the atmosphere (the so-called "air mass effect"), and the relative angle between the Sun's rays and collector. A solar-powered aircraft must fly above the altitude reached by clouds, which is usually around 14 km. Consideration of flying in the region of minimum wind velocity may dictate a still higher altitude. In the subsequent calculation, the assumption is made that the solar energy available is 1259 W/m^2 , which corresponds to the case of the Sun overhead at an altitude of 20 km. The variation of air mass attenuation with solar angle is neglected. The magnitude of this effect may be obtained from data in reference 10. Though the effect is large at sea level, it is only a few percent at altitudes above 20 km, where most of the calculations of the present report are made. In view of the uncertainties in other parameters, the neglect of this factor is believed to be justified.

Design features may be incorporated to maintain the solar collector normal to the Sun's rays. Some methods for accomplishing this result are discussed later in the report. As a result, the effect of solar angle with respect to the cells is neglected in the subsequent analysis.

Energy required. - The power-weight ratio required for level flight is determined by equations (21) and (15) by setting $\gamma = 0$ and $p = 1.0$. The power-weight ratio P_m/W_T is seen to depend on the variables C_L , C_D , c , ρ , and W_T/S . In the analysis presented herein, values are assumed for C_L , C_D , and c . The value of W_T/S is varied over a reasonable range, and several values of altitude, or ρ , are assumed. The energy required for level flight is simply the power multiplied by the time. The total energy-weight ratio E/W_T , which must be collected for 24 hr of operation is

$$\frac{E}{W_T} = \left(\frac{E}{W_T}\right)_{\text{day}} + \left(\frac{E}{W_T}\right)_{\text{night}} \quad (40)$$

The energy available for use at night is less than that used in charging the batteries in the day because of losses in charging and discharging the batteries. In this analysis, an efficiency of 0.8 is assumed for either charging or discharging. As a result, the value of $\left(\frac{E}{W_T}\right)_{\text{night}}$ is the actual energy required to fly divided by 0.64. The energy-weight ratio collected is then

$$\begin{aligned} \frac{E}{W_T} &= \left(\frac{P_m}{W_T}\right) (3600) \left[(24 - t_{\text{night}}) + \frac{t_{\text{night}}}{0.64} \right] \\ &= \frac{P_m}{W_T} (3600) \left[24 + t_{\text{night}} (0.5625) \right] \end{aligned} \quad (41)$$

The value of E/W_T may thus be calculated for any values of wing loading and altitude. The power which must be received by the solar cells is this total energy divided by the length of the day. This power is

$$\frac{P_c}{W_T} = \frac{E}{W_T} \left[\frac{1}{3600(24 - t_{\text{night}})} \right] \quad (42)$$

The weight of solar cells required is then

$$\frac{W_c}{W_T} = \frac{P_c/W_T}{(P/W)_c} \quad (43)$$

The ratio of solar-cell area to wing area is

$$\frac{S_c}{S} = \frac{\frac{W_c}{W_T} \frac{W_T}{S}}{(W/S)_c} \quad (44)$$

The motor weight is given by

$$\frac{W_m}{W_T} = \frac{P_m/W_T}{(P/W)_m} \quad (45)$$

The battery weight is given by

$$\frac{W_b}{W_T} = \frac{\left(\frac{E}{W_T} \right)_{\text{night}}}{(E/W)_b} = \frac{\frac{P_m}{W_T} (3600)t_{\text{night}}}{(E/W)_b} \quad (46)$$

Aircraft parameters. - In order to provide a basis for the calculations, values are assumed for the aircraft and equipment parameters based on estimates of the current state of technology. As mentioned previously, the effect of changes in these parameters may be easily determined. The values assumed are listed in table I. Two values of drag coefficient are assumed, 0.04046 and 0.07581, at a lift coefficient of 1.5. The lower value is representative of the capability of modern sailplanes, whereas the higher value is possibly more representative of that attainable with the low Reynolds number and light construction anticipated with solar-powered aircraft.

Calculation of length of night.- The value of t_{night} at the surface of the Earth may be calculated for any latitude and season by means of the equation (ref. 10)

$$t_{\text{night}} = 24 \left[1 - \frac{\cos^{-1} (\tan F \tan \delta)}{180} \right] \quad (47)$$

where δ , the component of tilt of the Earth's axis from a normal to the Sun-Earth line is $23.5 \sin (2\pi\tau/365)$ deg, τ is the time in days from the fall equinox, and F is the latitude angle. The following calculations were made for values of t_{night} of 12 hr and 16.3 hr, which correspond, respectively, to the spring and fall equinoxes at any location, and to the winter solstice at a latitude of 50.8° .

Presentation of results.- The various quantities calculated for the level-flight mode of operation are presented as functions of wing loading in figures 1 to 5 as follows:

	Figure
Total energy acquired by solar cells for 24 hr of flight per unit of vehicle weight	1
Ratio of area of solar cells to wing area	2
Ratio of weight of solar cells required to total weight	3
Ratio of motor weight to total weight	4
Ratio of battery weight to total weight	5

The values of total energy for 24 hr of flight (fig. 1) form the basis for the subsequent calculations of solar-cell area and battery weight. As shown by equation (21), the total energy increases as the square root of the wing loading and increases linearly with drag coefficient. Because the energy varies inversely as the square root of the air density, the energy required increases rapidly with increasing altitude.

The ratio of the weight of solar cells to total weight (fig. 2) varies as the square root of the wing loading and is always much less than 1.0 over the range of wing loading up to 100 N/m^2 . Therefore, the weight of solar cells does not place a limitation on the feasibility of the aircraft, even with values representative of current technology. The area of solar cells required, shown in figure 3, varies as the $3/2$ power of the wing loading. A solar-cell area equal to the wing area appears to be a reasonable upper limit without unduly compromising the aerodynamic or structural design.

The ratio of motor weight to total weight for level flight (fig. 4) is less than 0.05 for all conditions shown. The motor weight required does not depend on the length of the night.

The ratio of battery weight to total weight shown in figure 5, which assumes a battery capable of providing 24 278 J/N in the discharge cycle, exceeds 1.0 for all except the lighter wing loadings and lowest altitudes. This value, which is representative of current rechargeable batteries, therefore places a limit on the feasibility of solar-powered aircraft. Projected improvements in energy-storage systems using different approaches such as hydrogen-oxygen fuel cells give promise of reduction in weight by a factor of 10. The battery weight is also shown in figure 5 for a system capable of providing 242 780 J/N. This set of curves shows ratios of battery weight to total weight of less than 1.0 for most conditions investigated.

The curves of figure 6 show true airspeed as a function of wing loading for various values of altitude. These data are required to determine conditions under which the airspeed exceeds the wind velocity, a condition required for station keeping.

Region of feasible operation. - From the foregoing data, regions of feasibility may be determined for various combinations of design parameters. The possible limiting conditions are as follows:

- (1) Airspeed equals the wind speed.
- (2) Ratio of solar-cell area to wing area equals 1.0.
- (3) The sum of weights of the components equals the total weight corresponding to a given wing loading.
- (4) Mach number is sufficiently low to avoid aerodynamic losses. A Mach number of 0.3 is assumed to be a reasonable upper limit for flight at $C_L = 1.5$.

Examples of plots showing regions of feasibility determined from the data of figures 1 to 6 are presented in figure 7. Statistical data presented in reference 11 on winds at high altitude were used to determine the wing loading required for the flight speed at $C_L = 1.5$ to equal the wind speed. The data used are for 95-percentile winds in summer and winter conditions at Albuquerque, New Mexico.

In estimating weight limitations the following equation is used:

$$\frac{W_c}{W_T} + \frac{W_m}{W_T} + \frac{W_b}{W_T} + 0.3 = 1.0 \quad (48)$$

The value of 0.3 represents the assumed weight fraction of the structure and payload.

The curves of figure 7 show that the requirement for the airspeed to exceed the wind velocity places approximate lower limits on both the altitude of flight and on the wing loading. The altitude must be greater than 15 to 16 km in summer and 18 to 20 km in winter. These limits also give adequate clearance over clouds and weather. In addition,

the wing loading should be greater than about 12 N/m^2 in summer and 15 N/m^2 in winter. The upper limit of altitude is imposed by the weight condition, and the upper limit of wing loading is imposed by the solar-cell-area condition.

With the heavier battery weight assumed ($(E/W)_b = 24\ 278 \text{ J/N}$), there is no feasible region of flight even with the most efficient aerodynamic configuration and $t_{\text{night}} = 12 \text{ hr}$. With the storage system, however ($242\ 780 \text{ J/N}$), relatively large regions of feasible operation exist in summer conditions, and a smaller feasible region exists, even with the most unfavorable combination of aerodynamic efficiency, length of night, and winds.

Flight With Varying Altitude

Considerations of climb efficiency.- Inasmuch as the foregoing results show that the solar-powered aircraft flying at constant altitude is not feasible with currently available storage devices, an investigation of possible benefits from varying altitude appears desirable. By climbing during the day, energy can be stored as potential energy without the associated weight of an energy storage system. This benefit may be offset, however, by the increased weight of the motor and propulsive system required to provide the desired climb angle and the increased power or, alternatively, the larger wing area required to fly at higher altitude. In addition, aerodynamic efficiency may deteriorate because of the lower Reynolds number and higher Mach number associated with flight at higher altitudes.

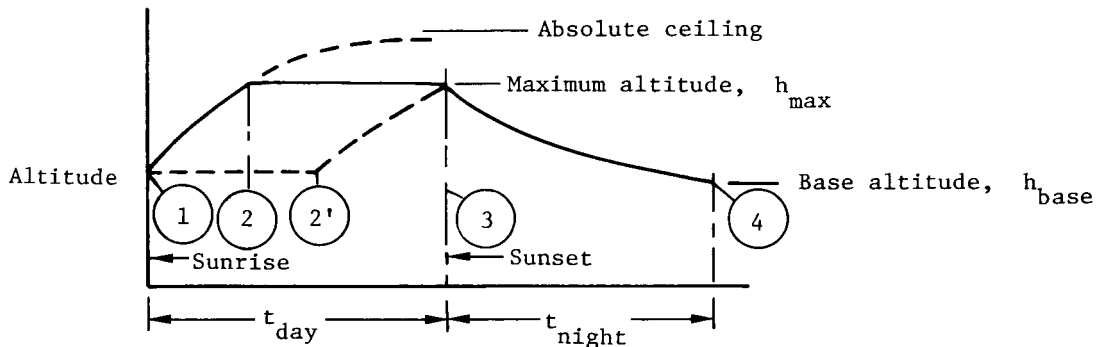
An important consideration in studying the effect of climbing is the climb efficiency, or ratio of energy stored as potential energy to the energy input to the propeller. By using equations (1), (5), and (15), the climb efficiency may be expressed in terms of C_D , C_L , c , γ , and C . If a parabolic drag polar is assumed, the value of C_D may be expressed in terms of $C_{D,0}$, C_L , and A (eq. (6)).

Plots showing the variation of climb efficiency η_c with flight-path angle γ for a number of typical cases are shown in figure 8. The contributions of the two factors, η and $1 - \frac{D}{T}$, which go to make up the climb efficiency, are also shown. For most cases, the climb efficiency is greatest at climb angles of 10° to 20° and remains remarkably constant at higher values of climb angle. The increase in the factor $1 - \frac{D}{T}$ with increasing climb angle tends to offset the decrease in propeller efficiency with increasing climb angle. Larger values of drag coefficient or larger values of c , the ratio of propeller diameter squared to wing area, cause the maximum climb efficiency to occur at larger values of climb angle. The maximum value of climb efficiency for typical values of airplane parameters is about 60 percent, which indicates that climbing is a relatively efficient way to store the propulsive energy of the motor, provided that the motor power is sufficient to provide a climb angle near or greater than the maximum of the curve of

climb efficiency. The curve presenting the effect of C_L shows that the best climb is usually at much lower values of C_L than that for a maximum value of $C_L^{3/2}/C_D$, which is the value for minimum sinking speed in a glide. For the standard case assumed in figure 8 ($C_{D,0} = 0.04$, $A = 20$), the maximum value of $C_L^{3/2}/C_D$ occurs at $C_L = 2.74$. The improved efficiency at lower values of lift coefficient results from the improved propeller efficiency at higher values of flight speed. This result depends on having enough power to produce the climb angles and airspeeds required.

Use of constant lift coefficient. - In subsequent calculations, the entire flight, including the climb, is assumed to take place at a constant value of lift coefficient. As shown previously, a somewhat greater rate of climb could be obtained by using a lower value of lift coefficient at high climb angles near the start of the climb. A comparison of the rates of climb using the optimum lift coefficient as compared with a constant lift coefficient for a typical case is shown in figure 9. The use of a constant lift coefficient ($C_L = 1.5$) is seen to reduce the rate of climb only slightly at 20 km, the lowest altitude considered; at the higher altitudes, the optimum rate of climb would require a lift coefficient which would probably exceed the maximum lift coefficient. The use of a constant lift coefficient in these calculations is therefore believed to be justified.

Flight profile without energy storage devices. - In order to investigate the performance obtained when energy is stored by climbing, a flight profile such as that shown in the following sketch is used:



The aircraft is assumed to operate between specified values of base altitude h_{base} and maximum altitude h_{max} . With these values given, the wing loading required to glide between points ③ and ④ in the time t_{night} is calculated from the value of K (eq. (28)), determined from equation (34) and/or (39), depending on whether the altitude range involved contains segments in which the temperature is constant or varies linearly with altitude. With this value of wing loading, the power required to fly at an absolute ceiling some specified height above the maximum altitude is calculated from equations (21) and (15). The climb in segment ①-② is assumed to take place at constant power. The power is the same as that which would be required to continue up to the absolute

ceiling specified previously. This power comes entirely from the solar cells. The solar-cell area and motor size required for this climb may therefore be determined. From the assumed equipment parameters given in table I, the ratios of weight of the solar cells and motor to total weight and the ratio of solar-cell area to wing area are determined from equations (43) to (45).

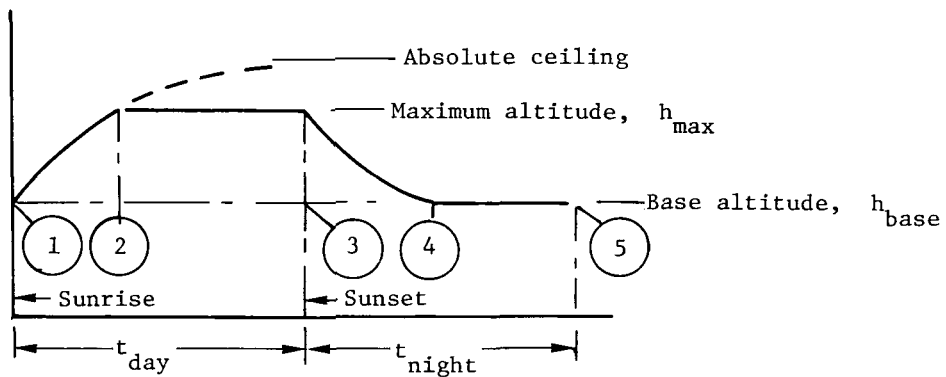
By using equation (24) and the methods in the section entitled "Calculation of Rate of Climb," the time to climb from h_{base} to h_{max} (segment ①-②) may be determined. The aircraft can then fly level in segment ②-③ using less than the full output of the solar cells, and some energy will be available to operate a payload. If the absolute ceiling were picked correctly, the aircraft could reach point ③ just as it reached h_{max} , and the required solar-cell area and motor weight would be minimized. This refinement is not included in the present calculations.

The energy available to operate a payload or to charge batteries might be increased somewhat by flying level during the day at h_{base} , as shown by the dashed line ①-②' in the sketch. The flight at higher altitude, however, takes the advantage of the higher true airspeed of the aircraft at high altitude and would allow greater capability to travel over the ground or to make progress into winds. This procedure was therefore assumed in these and subsequent calculations.

Presentation of results. - The results of the calculations for an aircraft which depends entirely on climbing to store energy are shown in figure 10. Figure 10(a) shows the required wing loading, power loading, and ratio of solar-cell area to wing area as a function of maximum altitude for $h_{\text{base}} = 20 \text{ km}$ and $t_{\text{night}} = 12 \text{ hr}$. Figure 10(b) shows the ratios of motor weight to total weight and the true airspeed at base altitude and maximum altitude. The wing loadings are seen to be extremely low, less than 1.7 N/m^2 even for $h_{\text{max}} = 45 \text{ km}$. These low wing loadings are far below those required to exceed the 95-percentile wind velocities at these altitudes. These designs are therefore not feasible. Furthermore, although there is no physical reason that such an aircraft could not fly with these low values of wing loading, the problem of handling and launching such a flimsy structure would be extremely difficult. The basic reason for the low wing loading required is the long length of the night. A time of 12 hr is 43 200 sec. Even with a value of sinking speed of 1 m/sec, typical of soaring gliders at sea level, the loss of altitude during the night would be 43.2 km. The low sinking speed required to remain above the base altitude this long in this high altitude region can be obtained only by using these unduly low values of wing loading.

Flight profile with energy storage devices. - Although problems are associated with the very low values of wing loading, the aircraft which are capable of remaining aloft by climbing and gliding require solar cells covering only a small fraction of the wing area to climb back to the maximum altitude in the daytime. As a result, batteries and

additional solar cells could be carried which would increase the wing loading and provide a higher airspeed. In order to study this possibility, the flight plan studied previously is modified as shown in the following sketch:



In segment ①-②, all power generated by the solar cells is assumed to be used for climbing, and in segment ②-③, the power is used to fly level and to charge the batteries. In segment ③-④, the aircraft glides with propeller folded, and in segment ④-⑤, it flies level using energy stored in the batteries.

In making the calculations, a series of values of wing loading are assumed. At each wing loading, the time required to glide from h_{\max} to h_{base} is calculated. The battery energy and weight required in segment ④-⑤ are then determined. The absolute ceiling is selected arbitrarily, and the time to climb at constant power (segment ①-②) and the required solar-cell area and motor weight to provide this power are determined. Finally, the energy to fly level in segment ②-③ and the energy remaining to charge the batteries are calculated. A check is made to determine whether the energy going into the batteries, reduced by the charge and discharge efficiencies, exceeds the energy required in segment ④-⑤. Any excess energy would be available for operating the payload. If the energy stored by the solar cells in segment ②-③ is less than that required in segment ④-⑤, however, the solar-cell area is recalculated to provide energy stored equal to that required. Again, the absolute ceiling could be picked so that the power received by the batteries in segment ②-③ just equaled that required in segment ④-⑤, but this refinement is not included in the present calculations.

Parameters assumed. - In the first set of calculations, the parameters assumed are the same as those in table I, but only $C_D = 0.07581$ is used. The base altitude is 20 km, and values of maximum altitude of 30, 35, 40, and 45 km are assumed. In each case, the absolute ceiling is taken as 10 km above the maximum altitude. The values of t_{night} are 12 hr and 16.3 hr.

In the second set of calculations, the parameters assumed are the same as those in table I, but only $C_D = 0.04046$ is used. The base altitude is 20 km, and values of

maximum altitude of 30, 35, and 40 km are assumed. The absolute ceiling is taken as 5 km above the maximum altitude. The values of t_{night} are 12 hr and 16.3 hr.

Presentation of results. - The various quantities calculated for the climb and descend mode of operation are shown as functions of wing loading in figures 11 to 16 as follows:

Quantity calculated	Figure	
	(a)	(b)
Energy acquired by batteries in segment ②-③ and energy which must be put in batteries to fly level in segment ④-⑤	11	14
Ratios of weights of motor, solar cells, and batteries to total weight	12	15
Ratio of solar-cell area to wing area	13	16

${}^a C_D = 0.07581$; ceiling over h_{max} 10 km.

${}^b C_D = 0.04046$; ceiling over h_{max} 5 km.

The results presented in these figures are largely self-explanatory. The energy going into the batteries in segment ②-③ must exceed that required for flight in segment ④-⑤. This condition is met in all cases in figure 11(a), and in all except the lowest value of h_{max} in figures 11(b) and 14(a). In figure 14(b), however, this condition is not met for any value of maximum altitude. In these cases, the solar-cell area is recalculated to supply the required energy in segment ④-⑤. With the increased area of solar cells, power would be available to climb more rapidly provided a larger motor were used. An iterative procedure could be used to find the solar-cell area and motor size so that the capability of the solar cells would be fully utilized both in the climb (segment ①-②) and in level flight (segment ②-③), but this refinement is not included in the present calculations. As a result, in most of the cases shown, some excess energy would be available to operate a payload.

Regions of feasible operation. - The results of the calculations for the climb and descend mode are summarized in figure 17 to show regions of feasible operation similar to those shown in figure 7 for the level-flight mode. In this case, the limits are shown for h_{max} plotted as a function of wing loading for a base altitude of 20 km.

The data of figure 17 show that with the lighter battery weight (242 780 J/N), there is a large feasible region of operation in the climb and descend mode for all conditions investigated. The weight condition in this case does not limit the region of feasible

operation because, at higher altitudes, the $M = 0.3$ boundary would be reached before the weight limitation. The maximum wing loading is again determined by the requirement for the ratio of solar-cell area to wing area to be less than 1.0.

With the heavier battery weight (24 278 J/N), there is again no feasible region of operation with the higher value of drag coefficient. With the lower value of drag coefficient, a small region exists with very high values of maximum altitude where the flight velocity exceeds the summer winds but not the winter winds. Also, the flight velocity at the base altitude is less than the wind velocity. Thus, there is a range of conditions in which the aircraft might be blown off station during segment ④-⑤ at night but could regain its position during the high-altitude segment ②-③ in the daytime. This possibility is indeed marginal because of the difficulty of obtaining a very efficient aerodynamic configuration at the high altitudes and low wing loadings involved.

DISCUSSION OF RESULTS

Effect of Changes in System Parameters

The presentation of data for weights and sizes of various power-plant components of the solar-powered aircraft as a function of wing loading makes it easy to determine the effect of changes in the characteristics of these components because the power required to fly in a given flight condition depends only on the wing loading and not on the characteristics of these components. For example, if the solar cells were 10 percent more efficient than the value assumed herein, the solar-cell area required at any value of wing loading would be 10 percent less. Similarly, the ratio of solar-cell weight to total weight could be modified in accordance with changes in the energy-weight ratio of the solar cells. New boundaries of regions of feasible operation could then be constructed.

Because of the rapidly changing state of the art in the technology of solar cells, batteries, and motors, the regions of feasible operation presented previously may be expected to change. Some important differences exist, however, in the magnitude of improvement which may be expected in the various technologies. These factors are discussed subsequently in the section entitled "Design Considerations."

Effect of Mode of Operation

Comparison of the level-flight mode of operation (fig. 7) with the climb and descend mode (fig. 17) shows that there is little difference in the required values of wing loading for the two modes. If level flight is conducted only at the minimum altitude set by the winds, say 20 km, somewhat higher values of wing loading are allowable because of the reduced motor size and solar-cell area required for level flight as compared with climb. By use of the climb and descend mode, however, a somewhat larger wing loading is

allowable with a maximum altitude of, say 30 km, than would be allowable for continuous level flight at this altitude. The margin of flight speed over the wind speed at this altitude is considerably greater than at 20 km which may be advantageous in providing flexibility of operation.

The ability to store some energy by climbing without the associated battery weight approximately offsets the increased power requirement of flight at higher altitude. In practice, a solar-powered aircraft would be operated in such a way as to take advantage of prevailing wind conditions. Because of the small or negligible penalty involved in providing a capability to climb to higher altitudes, the provision of such a capability in the design would probably be advantageous.

The adverse effect of the shorter period of daylight and longer night when operating in the winter at high latitudes is clearly shown in figures 7 and 17.

Design Considerations

Wing loading. - The most important design requirement for a solar-powered aircraft, as shown by the preceding calculations, is the need for a very light wing loading. The regions of feasible operations occur in the range of 15 to 30 N/m². This requirement results from the premise that the minimum altitude should be above the clouds and above the altitude at which the wind's velocity is likely to exceed the airspeed. The rapidly increasing average wind velocity and density below about 20 km tend to establish this value as a minimum altitude.

Though the values of wing loading required may seem extremely low by comparison with those of conventional airplanes, they are close to those demonstrated by successful man-powered airplanes (ref. 5). The "Gossamer Condor" for example, with a span of 29.3 m, had a ratio of structural weight to wing area of 4.66 N/m². This airplane would carry a concentrated load (the pilot) of more than twice the structural weight. In an unmanned aircraft of similar size, the solar cells and batteries could probably be distributed across the span so that a considerably lighter structural weight fraction would be possible. The payload capability of such an aircraft would still be quite small, however. For example, on a vehicle the size of the Gossamer Condor, with a wing area of 66.9 m² and loading of 15 N/m², a payload of 15 percent of the gross weight would amount to 150 N. The size of the aircraft cannot be increased arbitrarily to accommodate a larger payload because of the operation of the cube-square law. This law states that for geometrically similar structures of different sizes in vehicles of constant wing loading, all areas and loads vary as the square of the linear dimension. As a result, the stresses in the structural members are the same, but the structural weight varies as the cube of the linear dimension. Expressed in another way, the ratio of structural weight to wing area varies directly as the linear dimension. The structural weight fraction therefore

increases with increase in vehicle size. This law is usually overcome to some extent in larger conventional airplanes by use of lower load factors and more uniform distribution of load across the span. In the case of a solar-powered aircraft, however, full utilization of these features would probably be made regardless of size, so that the law would be more nearly followed. These considerations lead to the conclusion that the attainment of the light wing loadings required for solar-powered aircraft is facilitated by small size.

Solar-cell and battery technology.- The assumed characteristics of solar cells (table I) are readily attainable with current technology. Some improvements in efficiency and lighter weights are predicted to be possible by using improved manufacturing techniques and thinner materials. The overall improvement, however, would probably not result in more than double the energy per unit weight of the solar cells.

In the previous analysis, two values, differing by a factor of 10, were assumed for the specific energy capacity of batteries. These values represent two different technologies, namely, rechargeable batteries and fuel cells. The lower value of the energy capacity is attainable with existing rechargeable batteries, but this value has been shown to be inadequate for a practical solar-powered aircraft. On the other hand, the higher specific energy capacity projected for fuel cells has not as yet been demonstrated in practical hardware. The value assumed, however, is really considerably larger than necessary. Examination of the regions of feasibility (figs. 7 and 17) shows that with the larger specific energy capacity, the solar cells rather than the batteries place a limit on the feasible region of operation. An energy storage system with three to five times the specific energy capacity of that assumed for rechargeable batteries (72 800 to 121 000 J/N) would be adequate and would make a solar-powered aircraft practical.

Motor technology.- The assumed specific power of the motor, 168 W/N, is high for current technology, particularly if the weight of the gearing and propeller is included with the motor. The weight of the motor, however, is far smaller than that of the solar cells and batteries so that changes in the value of this parameter do not affect the design very much.

Aerodynamics.- The attainment of high aerodynamic efficiency at high values of lift coefficient requires a low subsonic Mach number and a sufficiently high Reynolds number. A value of Mach number of 0.3 is suggested as a reasonable upper limit because of the increased velocity of the propeller tips as compared with the flight speed. The Mach number and Reynolds number per meter chord are plotted in figure 18 as a function of wing loading for a lift coefficient of 1.5 and various values of altitude. Figure 18 shows that, for values of wing loading below 40 N/m², the Mach number limit of 0.3 is not encountered below an altitude of about 38 km. Reynolds number based on mean chord may also be expressed as a function of vehicle gross weight for various values of the

product of lift coefficient and aspect ratio $C_L A$. A plot of this type, based on the equation presented in the figure, is given in figure 19.

The aerodynamic efficiency of manned soaring gliders operating in a range of Reynolds number from 1×10^6 to 4×10^6 is very high, but as the Reynolds number decreases, the attainable section lift-drag ratio decreases gradually because of the increased skin-friction coefficients for both laminar and turbulent boundary layers at lower Reynolds numbers. At still lower values of Reynolds number, the efficiency decreases further because of the formation of laminar separation bubbles. Below some value of Reynolds number, sometimes called the critical Reynolds number for the airfoil, extensive laminar separation occurs which results in a very poor aerodynamic efficiency. This critical Reynolds number may be in the range of 6×10^4 to 2×10^4 for airfoils designed especially for low Reynolds numbers (ref. 12). In order to obtain a reasonably high section lift-drag ratio, a minimum value of Reynolds number of about 1.5×10^5 appears desirable.

As shown in figure 19, rather large values of wing chord, and hence large aircraft, are required to provide this value of Reynolds number at altitudes above 20 km. In the previous calculations, values of C_L of 1.5 and A of 20 and 35 were assumed, giving values of $C_L A$ of 30 and 52.5. The values of aircraft weight, area, and wing span required to provide a Reynolds number of 1.5×10^5 , as obtained from figure 19, are shown in the following table:

$C_L A$	Altitude, km	Weight, N	Wing area, m ² (a)	Wing span, m (a)
30	20	785	39.3	28.0
	25	1800	90.0	42.4
	30	4100	205	64.0
52.5	20	1350	67.5	48.6
	25	3160	158	74.4
	30	7080	354	111

^aValues based on $W_T/S = 20 \text{ N/m}^2$.

This table shows that, from the standpoint of aerodynamic efficiency, a solar-powered aircraft should be large. The required size increases rapidly with increased operating altitude.

Practical Aspects of Design of a Solar-Powered Aircraft

Size, structural weight, and loading conditions. - In considering the boundaries of feasible operation shown in figures 7 and 17, it should be realized that at the upper right-hand boundaries determined by the condition $\sum W = 1$, all the capability of the vehicle is used in lifting its power plant, except for the weight fraction of 0.3 allowed for the sum of structure and payload. Likewise, on the boundary $S_c/S = 1$, the entire wing area must be covered by solar cells simply to fly the vehicle. In the lower left-hand part of the region of feasible operation, however, additional capability exists for carrying payload, and the solar-cell area may be reduced or used for supplying energy to a payload. In practice, therefore, the wing loading should be as low as possible. The minimum wing loading is determined solely by the need to provide an airspeed greater than the wind velocity. The boundaries shown are for the 95-percentile wind data. If the aircraft is not required to maintain station such a large fraction of the operating time, still lower values of wing loading may be used.

The discussion in the section entitled "Aerodynamics" indicates that a large vehicle is required at these low values of wing loading to attain the necessary Reynolds number, whereas consideration of the cube-square law indicates that the structural weight fraction may become excessive beyond some vehicle size. If the payload weight is not specified a priori, there is probably an optimum vehicle size representing the best compromise between these conflicting requirements. The best available baseline for judging the ability to make a sufficiently light structure is probably the successful man-powered vehicle described in reference 5. This externally braced vehicle had a wing loading of 14.4 N/m², carried a concentrated load, and had a structural weight fraction of about 0.3 with a span of 29.3 m. As pointed out previously, the structural weight fraction could probably be reduced considerably by distributing the load across the span. This example indicates, therefore, that some of the larger vehicles in the preceding table could probably be constructed with a sufficiently low weight fraction.

The loading conditions required for the design of such a large light structure with the load distributed fairly uniformly across the span present an interesting subject for research. Bending moments produced by a uniform gust load would be small. The effect of varying gust velocity across the span might become critical for the design. In addition, considerations of handling and launching the vehicle might impose loading conditions more severe than flight loads. Further discussion of these problems is beyond the scope of this report.

Solar-cell arrangement. - In the preceding analysis, the assumption is made that the power available from the solar cells is constant throughout the daylight hours. This assumption implies that the solar cells may be kept normal to the Sun line. This capability is desirable because the power available decreases approximately as the cosine of

the angle from the normal to the plane of the solar cells. The angle of the Sun's rays above the horizon, of course, varies from some maximum value at midday to zero at sunrise and sunset.

One way to maintain the solar cells normal to the Sun line is to mount the cells on a tilting platform enclosed in a fuselage or pod covered with transparent material. The azimuth angle of the cells can then be adjusted by the heading of the aircraft and the elevation by the tilt of the solar-cell arrays. This method may be possible because, as shown in figures 2 and 13, when the wing loading is near the minimum value set by the wind velocity, the solar-cell area required is much less than the wing area. Some provision for cooling internal solar cells might be needed, however, resulting in a weight and drag penalty.

Another way to adjust the tilt of the solar cells in elevation is to mount them on the upper surface of the wing and bank the aircraft so that the normal to the wing lies along the Sun line. A conventional airplane cannot maintain straight flight at a large bank angle. By use of a cruciform arrangement of wings as illustrated in figure 20(a), with only one wing equipped with solar cells, the aircraft can bank so that the solar cells face the Sun while maintaining straight flight. Station keeping may be performed by flying a racetrack pattern, banking first in one direction, then the other.

If the aircraft were required to maintain an equivalent constant power output during daylight hours without changing the tilt of the solar cells, cells would have to be mounted on both sides of the aircraft as well as on the top of the wing. About three times the area of solar cells would be required as compared with the methods which allow tilting the cells. Inasmuch as the weight and cost of solar cells are important factors in the design of a solar-powered aircraft, the methods which allow tilting the cells are believed to be advantageous.

The use of the cruciform wing arrangement, of course, involves aerodynamic penalties. As shown in the analysis given in the appendix, the lift and induced drag of a cruciform wing are independent of the roll angle for a given angle of attack of the roll axis and are equal to these quantities for a horizontal monoplane of the same span. The profile drag of the cruciform wing, however, is twice that of the monoplane. One method to partially offset this increase in profile drag is to eliminate the fuselage and tail, as illustrated in figure 20(b). Pitching and yawing moments required for control and stability are provided by differential thrust of propellers mounted near the wing tips. Further studies are required to determine the relative merits of these and other methods for improving the performance of solar-powered aircraft.

CONCLUDING REMARKS

Because an actual solar-powered aircraft capable of staying aloft overnight has not yet been produced, studies must be based on estimates of the state of the art of the propulsion, structure, and aerodynamic technologies involved. These factors may be expected to change in the future. For this reason, the present report has been written to allow design studies to be made incorporating any desired values of these parameters. A number of theoretical developments are presented for calculating the climb, level flight, and descent performance of a solar-powered aircraft. Weights and sizes of the propulsion components are presented as functions of wing loading for level flight and for a climb and descend mode of operation. These charts are used to calculate regions of feasible operation in terms of altitude and wing loading with reasonable values of the system parameters. Conclusions reached in this study are

1. The wing loading of a solar-powered aircraft should be as low as possible. The requirement for the flight speed to exceed the wind speed sets a minimum value of wing loading of about 15 N/m^2 and a minimum altitude of about 20 km.
2. Presently available solar cells are adequate to provide operation of a solar-powered aircraft over a reasonable range of values of altitude and wing loading.
3. A flight plan consisting of climbing to store energy in the daytime and gliding at night is not feasible because, with the minimum values of wing loading and altitude stated previously, the altitude lost during the night is much too great.
4. If energy is stored in batteries, the operation of a solar-powered aircraft with presently available rechargeable batteries is not feasible because of the excessive weight of the batteries. Operation appears feasible, however, with the projected specific energy of other energy storage systems.
5. In order to obtain a sufficiently high value of Reynolds number for adequate aerodynamic efficiency, a solar-powered aircraft must be large, with a wing span in the range of 30 to 110 m, depending on the operating altitude. A problem may exist in obtaining a sufficiently low structural weight fraction at the larger sizes. Despite the large size, the payload capability is quite modest because of the very low wing loading.
6. The conditions of winter at high latitudes are very unfavorable for the operation of a solar-powered aircraft because of the shorter days and longer nights and because of the higher average winds in winter.

Langley Research Center
National Aeronautics and Space Administration
Hampton, VA 23665
April 11, 1980

APPENDIX

ANALYSIS OF LIFT AND INDUCED DRAG OF A CRUCIFORM WING AT VARIOUS ROLL ANGLES

A brief analysis is presented of the lift and induced drag of a cruciform wing at various roll angles.

Symbols

$D_{i,H}$	induced drag of normally horizontal wing
$D_{i,V}$	induced drag of normally vertical wing
K	ratio of induced drag to square of lift
L_H	lift of normally horizontal wing
L_O	reference value of lift (value of lift of one wing in horizontal orientation)
L_V	lift of normally vertical wing
V	vertical force developed by wing system
ϕ	angle of roll of wing system

Analyses

Consider a cruciform wing of high aspect ratio rolled about an axis which is tilted in a vertical plane with respect to the airstream. The zero lift lines of the wings are assumed to be aligned with this axis. The lift of each wing normal to its span is as follows:

$$L_H = L_O \cos \phi$$

$$L_V = L_O \sin \phi$$

Taking vertical components of these lift forces gives the vertical force of the combination

$$V = L_H \cos \phi + L_V \sin \phi$$

$$V = L_O (\cos^2 \phi + \sin^2 \phi) = L_O$$

APPENDIX

Thus, the lift is independent of the bank angle for a given tilt of the roll axis. At a bank angle of 45° , the angle of attack of each wing is only 0.707 times that of the horizontal wing at $\phi = 0^\circ$. The cruciform wing will therefore develop a higher value of maximum lift when $\phi = 45^\circ$ than when $\phi = 0^\circ$.

The velocities induced on one wing by the flow field of the other wing are in a span-wise direction and, to the first approximation, have no effect on lift or drag. The induced drag of each wing is proportional to the square of its lift. Thus,

$$D_{i,H} = KL_H^2 = KL_0^2 \cos^2 \phi$$

$$D_{i,V} = KL_V^2 = KL_0^2 \sin^2 \phi$$

The total induced drag is therefore

$$D_{i,H} + D_{i,V} = KL_0^2 (\cos^2 \phi + \sin^2 \phi) = KL_0^2$$

Thus the induced drag of the cruciform wing is independent of bank angle for a given tilt of the roll axis.

REFERENCES

1. Irving, F. G.; and Morgan, D.: The Feasibility of an Aircraft Propelled by Solar Energy. AIAA Paper No. 74-1042, Sept. 1974.
2. Boucher, R. J.: Project Sunrise. AIAA Paper 79-1264, June 1979.
3. Chinn, P. G. F.: Foreign Notes. Model Airplane News, vol. 94, no. 1, Jan. 1977, pp. 6, 8, 104, and 105.
4. UK's First Solar Aircraft Takes Off. Flight Int., vol. 115, no. 3667, June 30, 1979, p. 2336.
5. MacCready, Paul B.: Flight on 0.33 Horsepower: The Gossamer Condor. AIAA Paper 78-308, Feb. 1978.
6. Velupillai, David; and Hall, Tim: Gossamer Albatross - Anatomy of a Cross-Channel Flier. Flight Int., vol. 116, no. 3671, July 28, 1979, pp. 258-262.
7. Youngblood, James W.; Darnell, Wayne L.; Johnson, Robert W.; and Harriss, Robert C.: Airborne Spacecraft - A Remotely Powered, High-Altitude RPV for Environmental Applications. NASA paper presented at Electronics and Aerospace Systems Conference (Arlington, Virginia), Oct. 9-11, 1979.
8. Glauert, H.: The Elements of Aerofoil and Airscrew Theory. Second ed. Cambridge Univ. Press, 1947. (Reprinted 1948.)
9. U.S. Standard Atmosphere, 1962. NASA, U.S. Air Force, and U.S. Weather Bur., Dec. 1962.
10. Kreider, Jan F.; and Kreith, Frank: Solar Heating and Cooling: Engineering, Practical Design, and Economics. Rev. first ed., Hemisphere Pub. Corp., c.1977, p. 47.
11. Strganac, Thomas W.: Wind Study for High Altitude Platform Design. NASA RP-1044, 1979.
12. Carmichael, Bruce H.: A Significant Increase in Lift to Drag Ratio of Airfoils at Low Reynolds Number Through the Use of Multiple Trippers and Low Drag Laminar Flow. Natl. Free Flight Soc. Symposium, 1978, pp. 14-20.

TABLE I. - VALUES OF PARAMETERS USED IN CALCULATIONS

Aircraft parameters:

C_L	1.5
${}^a C_D$	0.07581, 0.04046
c	0.4
C	0.1

Energy system parameters:

Motor

$\left(\frac{P}{W}\right)_m$	167.64 W/N
--	------------

Batteries

$\left(\frac{E}{W}\right)_b$	24 278 J/N or 242 780 J/N
--	---------------------------

Solar cells

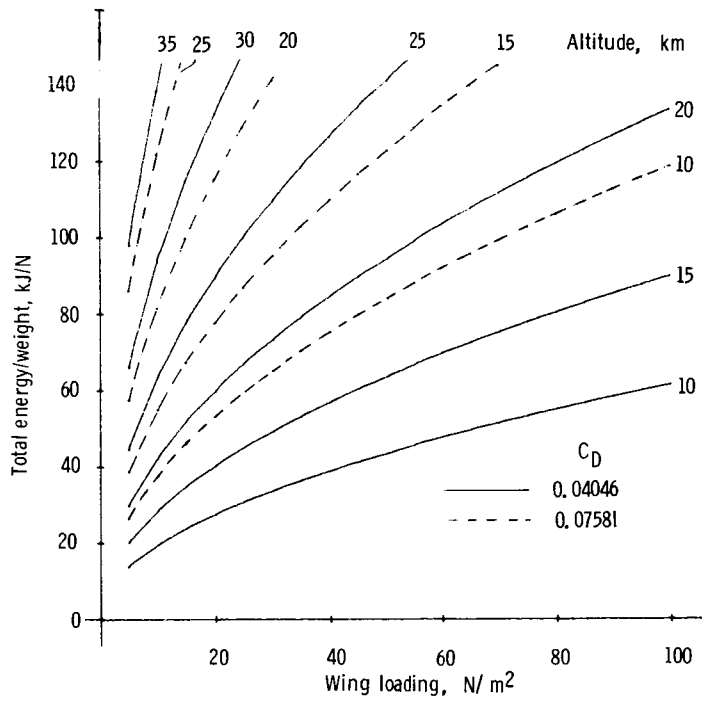
$\left(\frac{P}{W}\right)_c$	18.045 W/N
${}^b \left(\frac{P}{S}\right)_c$	129.6 W/m ²
$\left(\frac{W}{S}\right)_c$	7.182 N/m ²

$${}^a C_D = C_{D,o} + C_L^2 / \pi A.$$

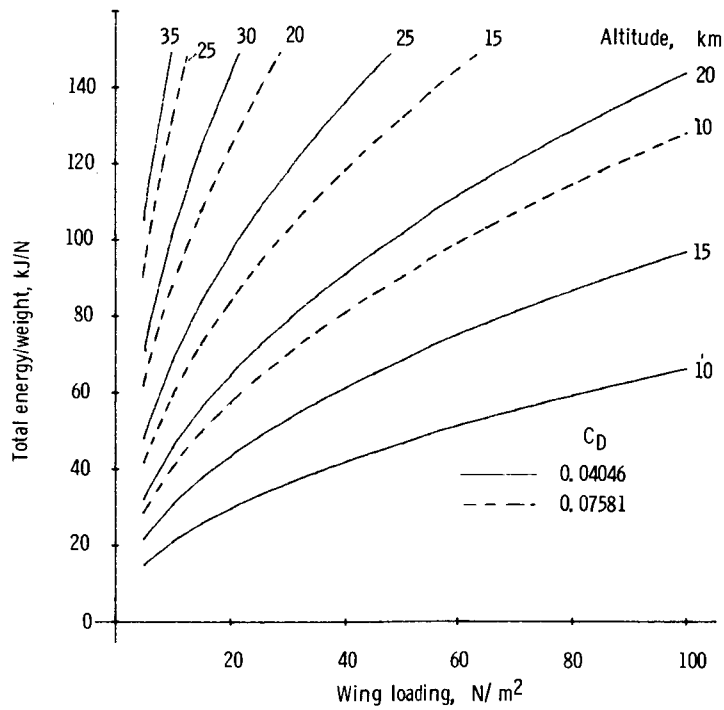
For $C_D = 0.07581$, $C_{D,o} = 0.04$ and $A = 20$

For $C_D = 0.04046$, $C_{D,o} = 0.02$ and $A = 35$

^bSolar radiation at 20 km assumed 1259 W/m²; solar-cell efficiency assumed 10.29 percent, including losses in wiring.

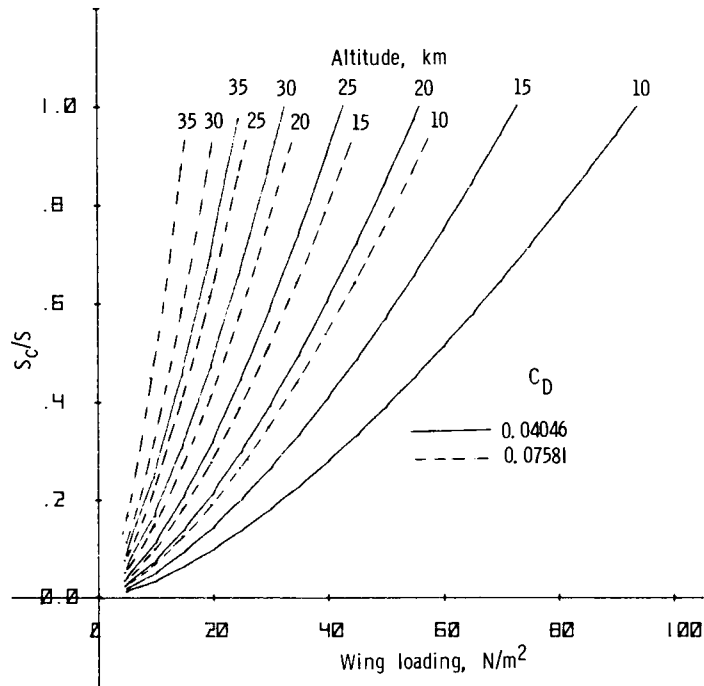


(a) $t_{\text{night}} = 12$ hr.

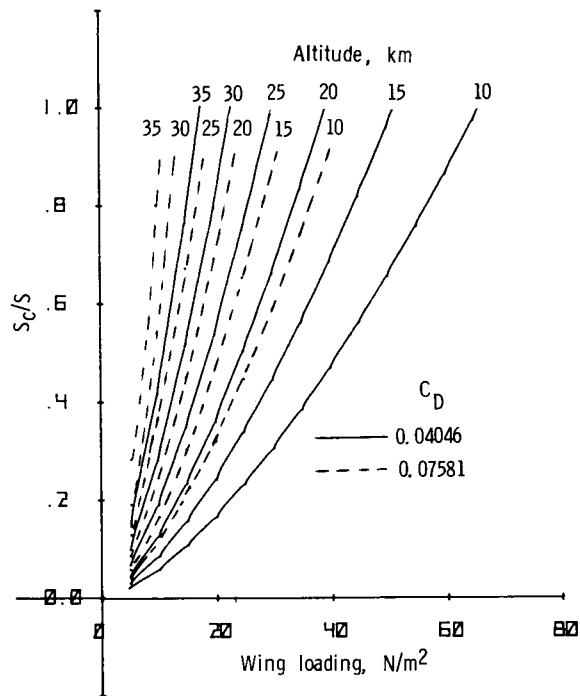


(b) $t_{\text{night}} = 16.3$ hr.

Figure 1.- Total energy acquired by solar cells during day for 24 hr of flight per unit of vehicle weight as function of wing loading. Flight at constant altitude; $C_L = 1.5$.

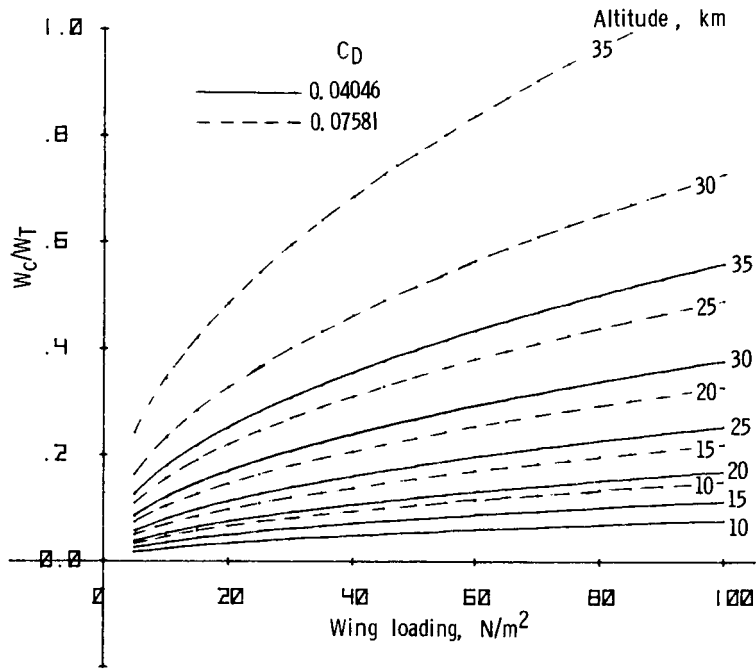


(a) $t_{\text{night}} = 12$ hr.

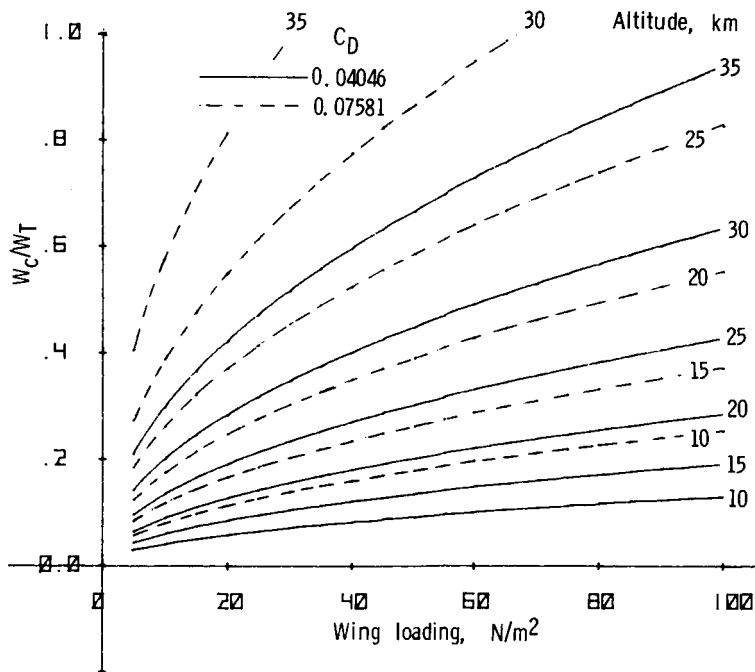


(b) $t_{\text{night}} = 16.3$ hr.

Figure 2.- Ratio of area of solar cells to wing area as function of wing loading.
Flight at constant altitude; $C_L = 1.5$.



(a) $t_{\text{night}} = 12 \text{ hr.}$



(b) $t_{\text{night}} = 16.3 \text{ hr.}$

Figure 3.- Ratio of weight of solar cells to total weight as function of wing loading.
Flight at constant altitude; $C_L = 1.5$.

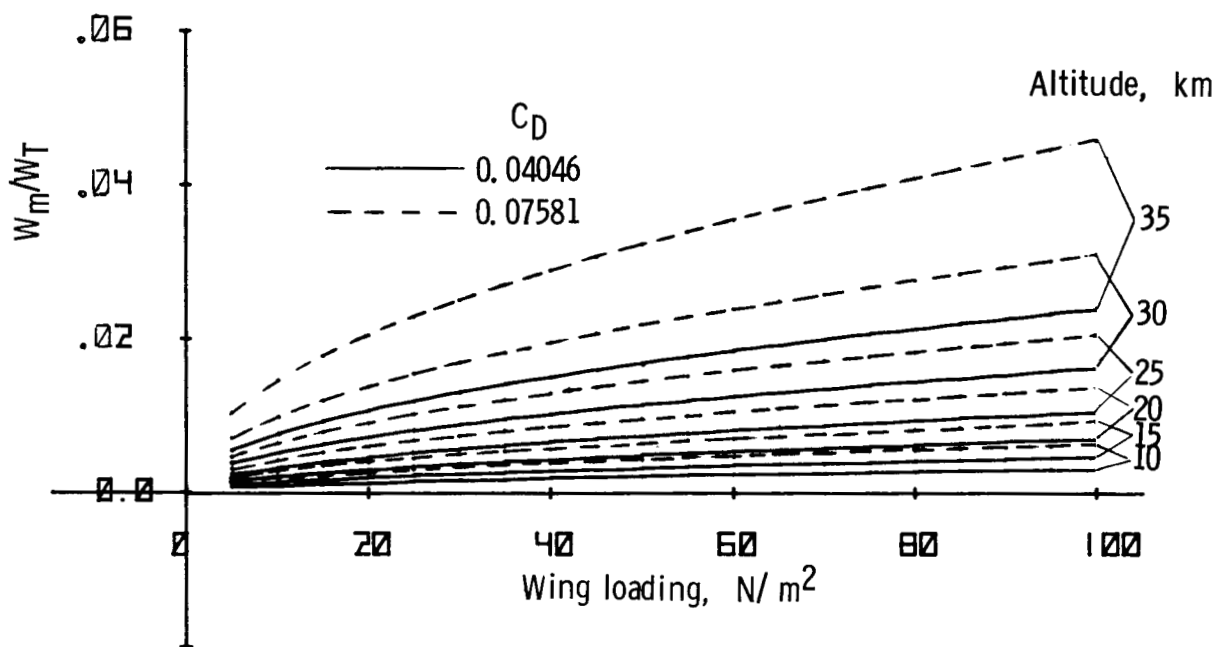
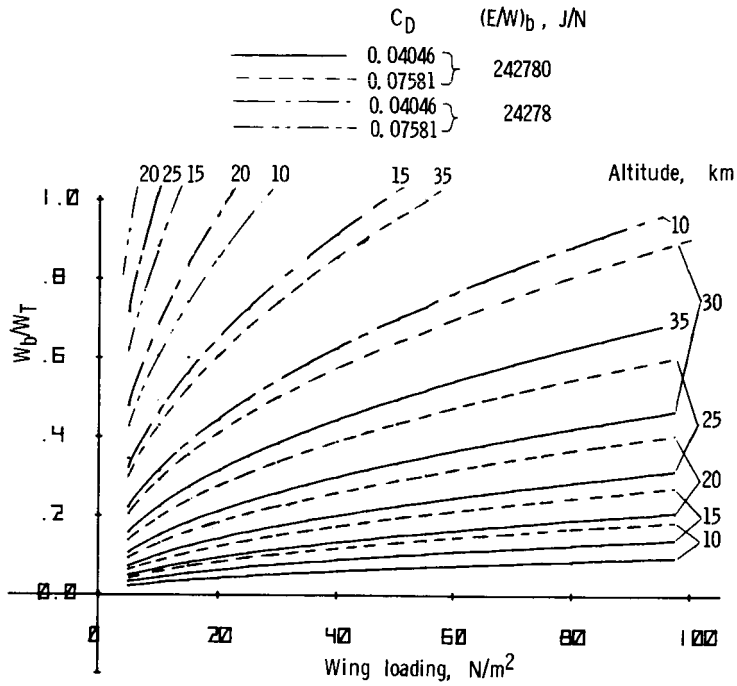
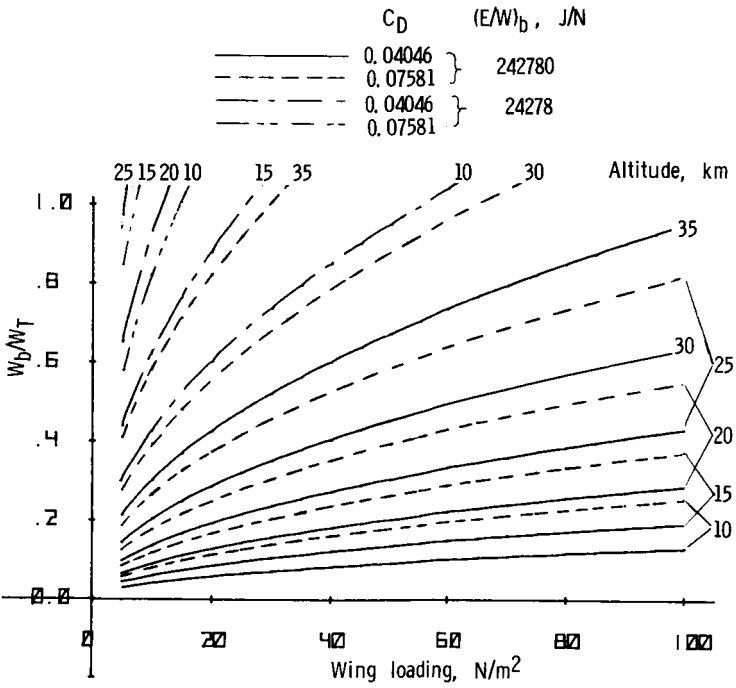


Figure 4.- Ratio of motor weight to total weight as function of wing loading.
 Flight at constant altitude; $C_L = 1.5$. Values are independent of t_{night} .



(a) $t_{\text{night}} = 12 \text{ hr.}$



(b) $t_{\text{night}} = 16.3 \text{ hr.}$

Figure 5.- Ratio of battery weight to total weight as function of wing loading. Flight at constant altitude; $C_L = 1.5$. Data shown for two values of battery specific energy and two values of drag coefficient.

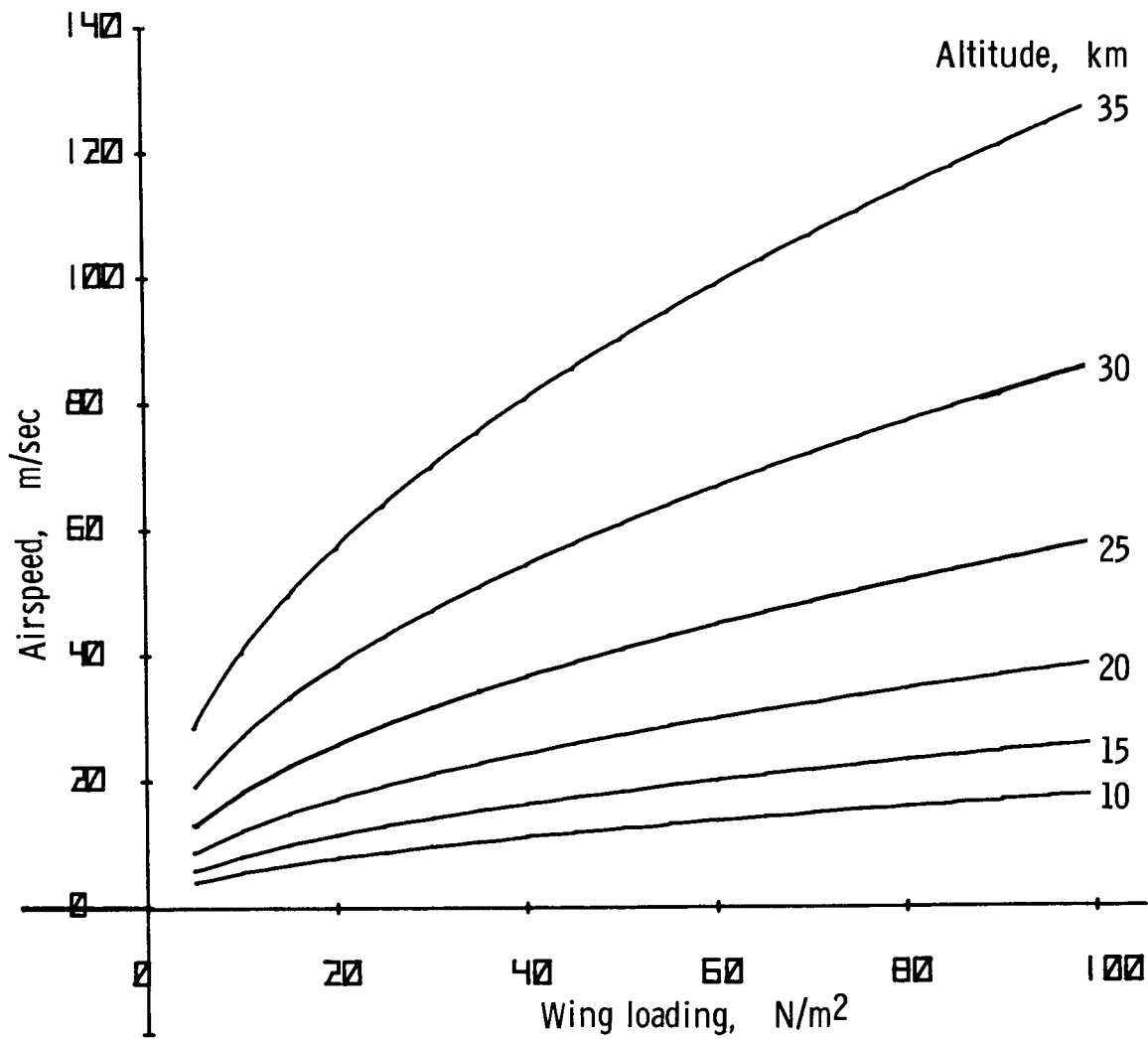
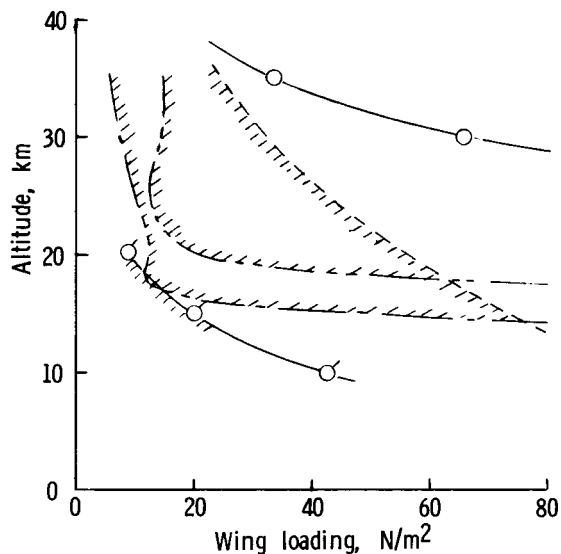
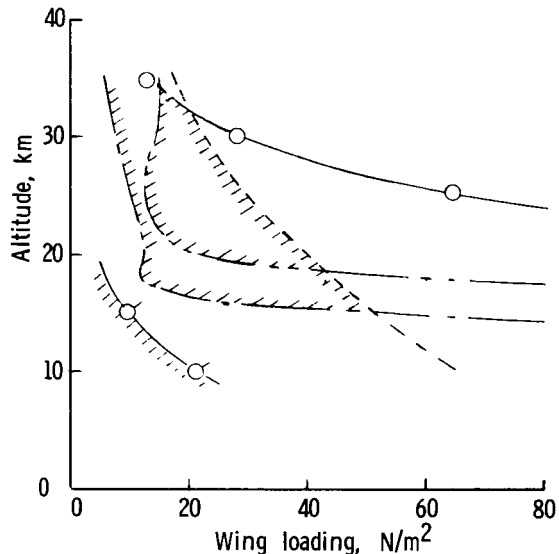


Figure 6.- True airspeed as function of wing loading at various values of altitude. $C_L = 1.5$.

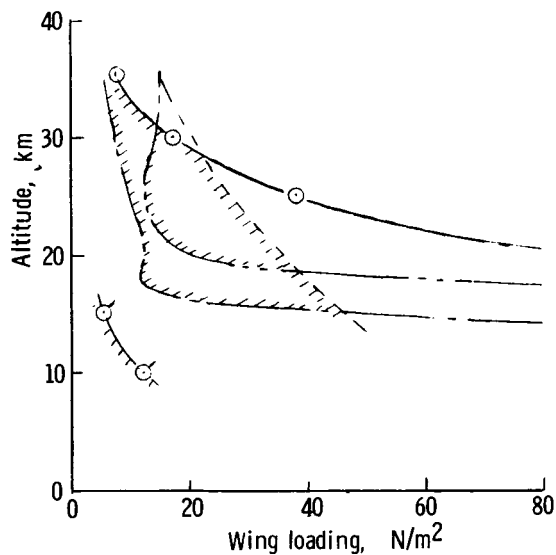
—○— $\Sigma W = 1, (E/W)_b = 242\ 780\ \text{J/N}$
 -○- $\Sigma W = 1, (E/W)_b = 24\ 278\ \text{J/N}$
 - - - $S_c/S = 1$
 - - - Winds (summer)
 - - - Winds (winter)



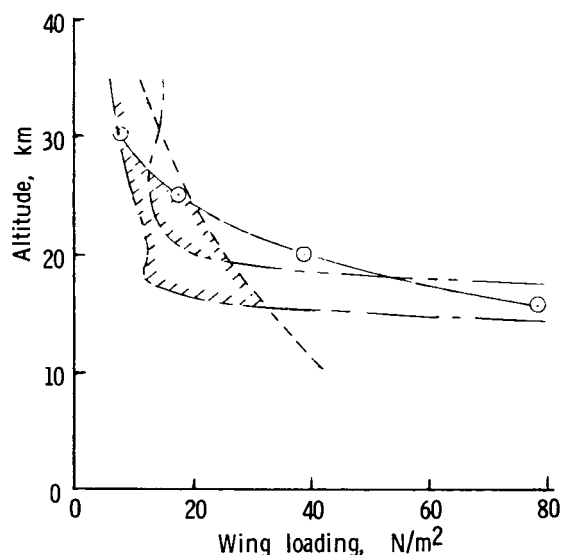
(a) $C_D = 0.04046$; $t_{\text{night}} = 12\ \text{hr}$.



(b) $C_D = 0.04046$; $t_{\text{night}} = 16.3\ \text{hr}$.

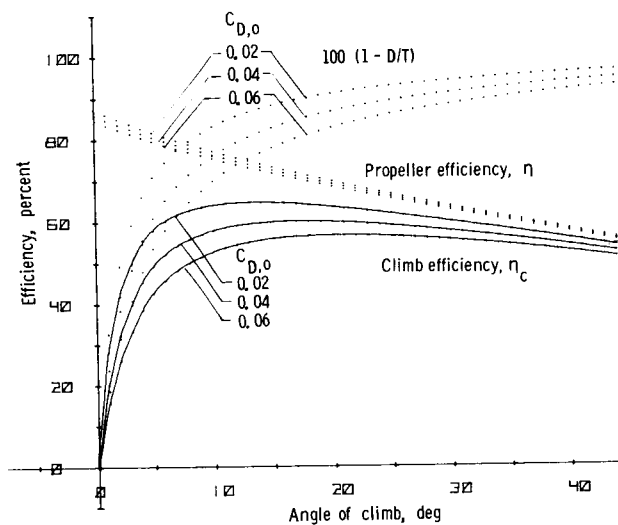


(c) $C_D = 0.07581$; $t_{\text{night}} = 12\ \text{hr}$.

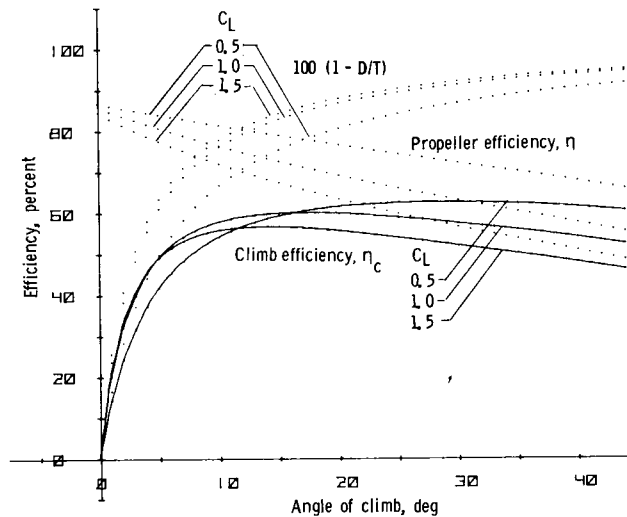


(d) $C_D = 0.07581$; $t_{\text{night}} = 16.3\ \text{hr}$.

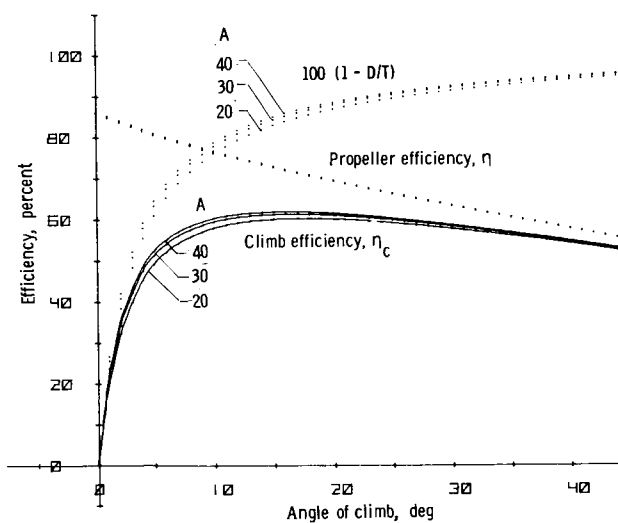
Figure 7. - Regions of feasible operation in level flight. $C_L = 1.5$.



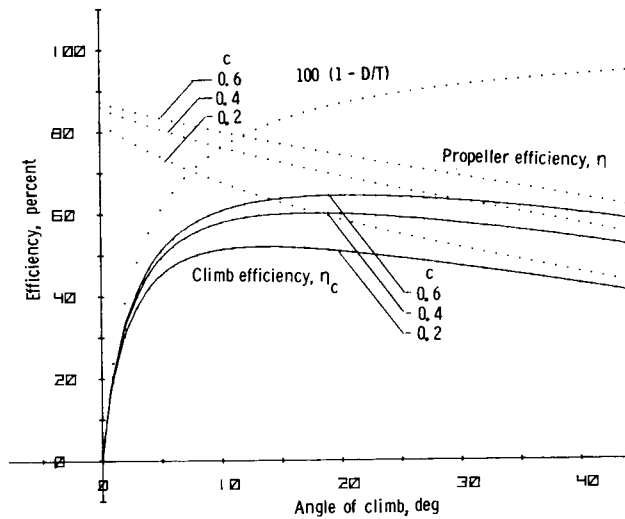
(a) Effect of profile drag coefficient $C_{D,0}$.



(b) Effect of lift coefficient C_L .



(c) Effect of aspect ratio A .



(d) Effect of propeller area ratio c .

Figure 8.- Variation of climb efficiency η_c with flight-path angle γ for a number of different conditions. Unless otherwise noted, $C_{D,0} = 0.04$; $C_L = 1.0$; $A = 20$; $c = 0.4$.

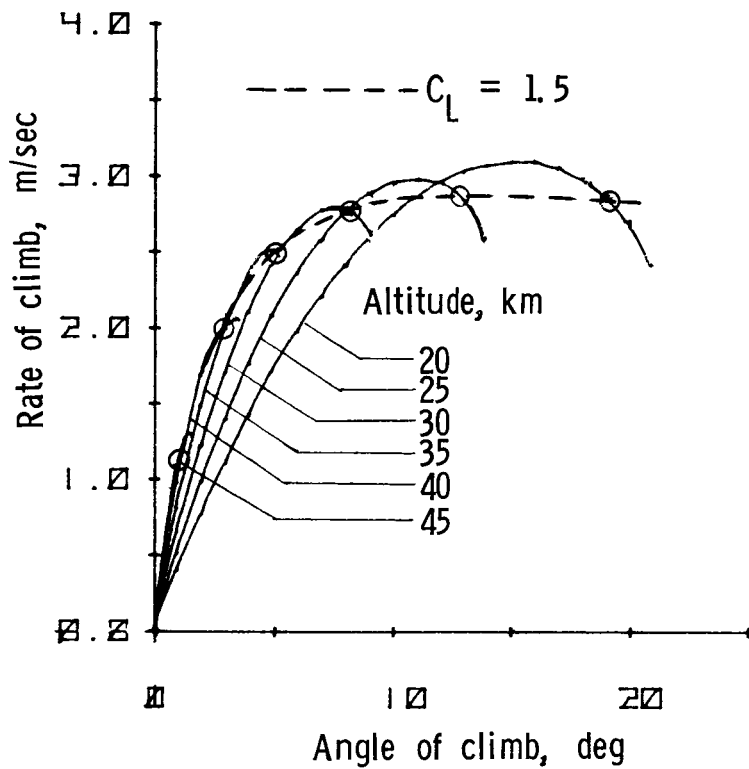
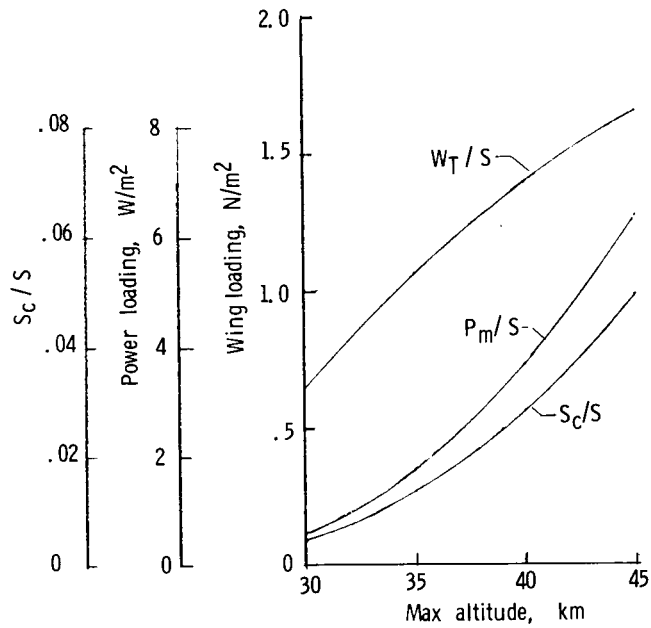
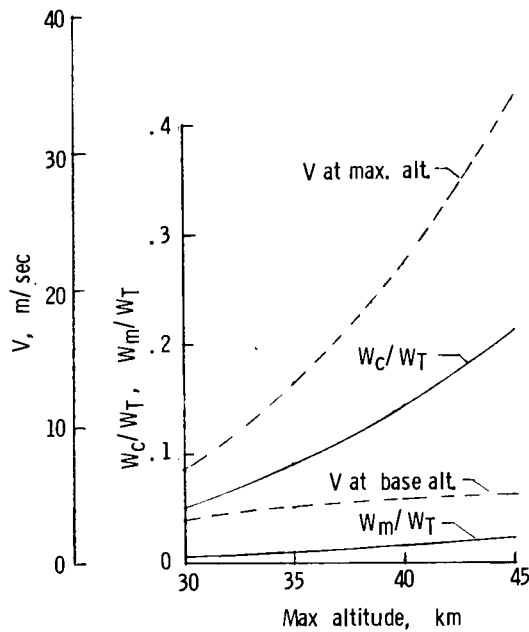


Figure 9.- Rate of climb as function of angle of climb for various altitudes. The dashed line connects points at $C_L = 1.5$; $W_T/S = 5.39 \text{ N/m}^2$; $C_{D,0} = 0.04$; $P_m/W_T = 5.13 \text{ W/N}$; $D = 0.4$; $A = 20$. At each altitude, the rate of climb at $C_L = 1.5$ is only slightly less than that at optimum value of C_L .

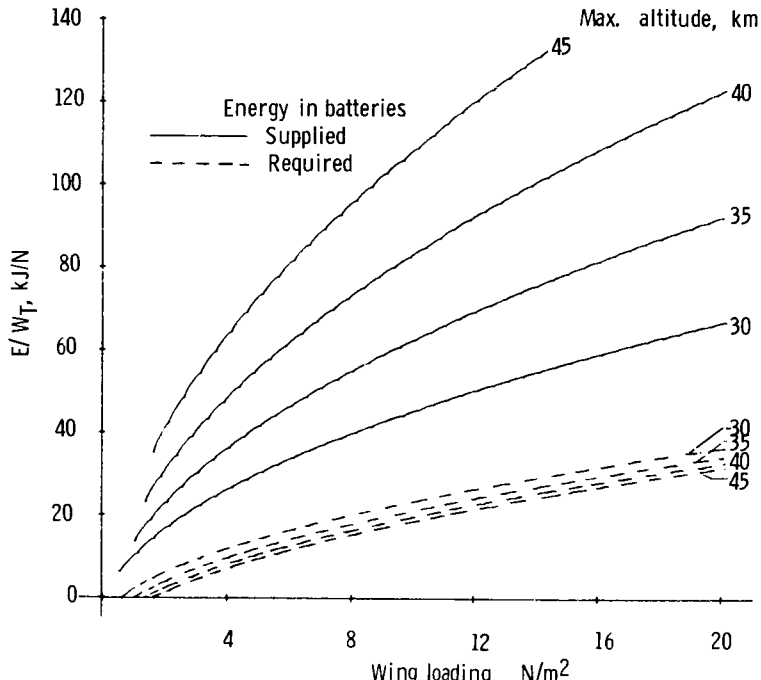


(a) Wing loading, power loading, and ratio of solar-cell area to wing area.

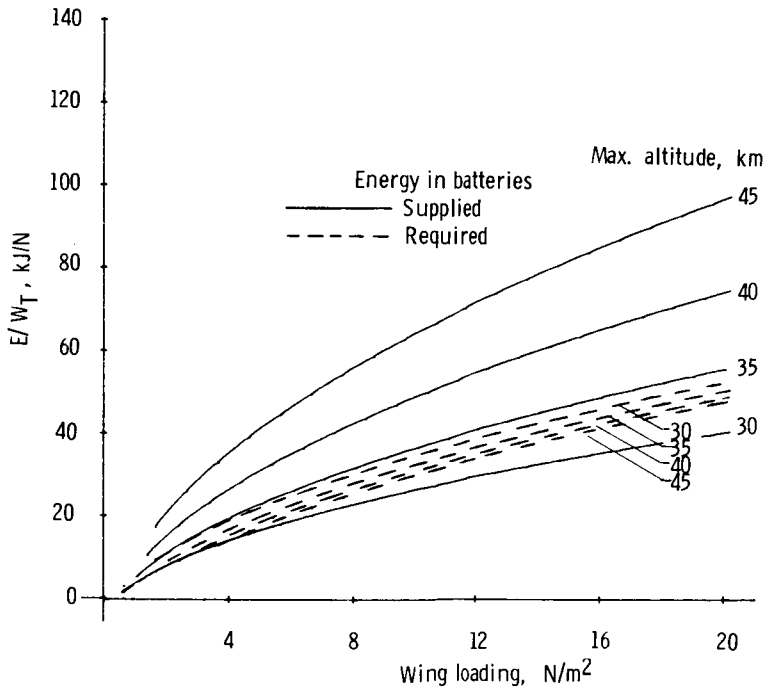


(b) Ratios of weights of solar cells and of motor to total weight, and airspeed at base altitude and at maximum altitude.

Figure 10.- Aircraft parameters for a solar-powered aircraft which stores energy by climbing. Parameters are plotted as function of maximum altitude for base altitude of 20 km. The wing loading is that required to glide from maximum altitude to base altitude in 12 hr. The power is that required to provide an absolute ceiling 10 km above the maximum altitude. Climb back from base altitude to maximum altitude requires less than 12 hr.

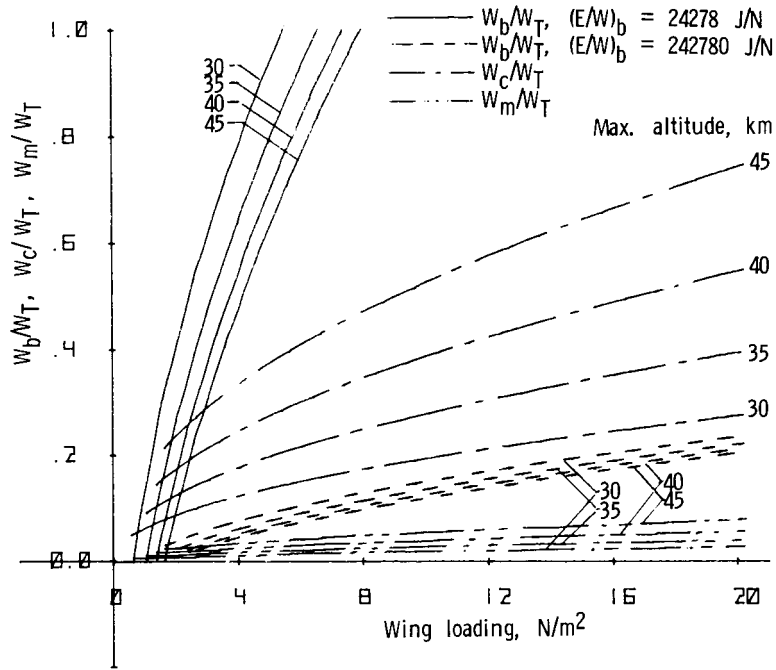


(a) $t_{\text{night}} = 12 \text{ hr.}$

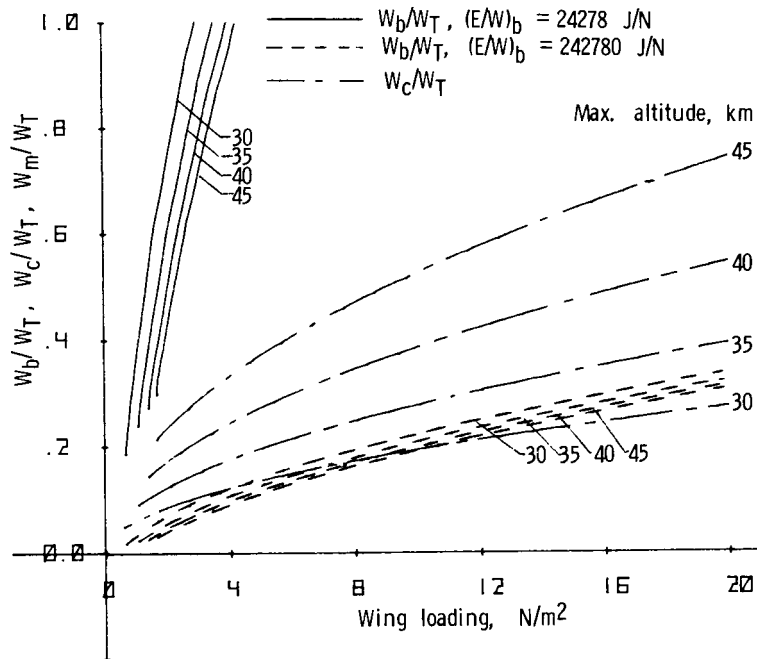


(b) $t_{\text{night}} = 16.3 \text{ hr.}$

Figure 11.- Energy per unit total weight supplied to batteries in segment ②-③ and required for level flight in segment ④-⑤ as function of wing loading for climb and descend mode of operation. Base altitude = 20 km; $C_L = 1.5$; $C_D = 0.07581$. Absolute ceiling 10 km above maximum altitude.



(a) $t_{\text{night}} = 12 \text{ hr.}$



(b) $t_{\text{night}} = 16.3 \text{ hr.}$

Figure 12.- Ratios of weights of motor, solar cells, and batteries to total weight as functions of wing loading for climb and descend mode of operation. Base altitude = 20 km; $C_L = 1.5$; $C_D = 0.07581$. Absolute ceiling 10 km above maximum altitude. Motor weight and solar-cell weight are independent of t_{night} .

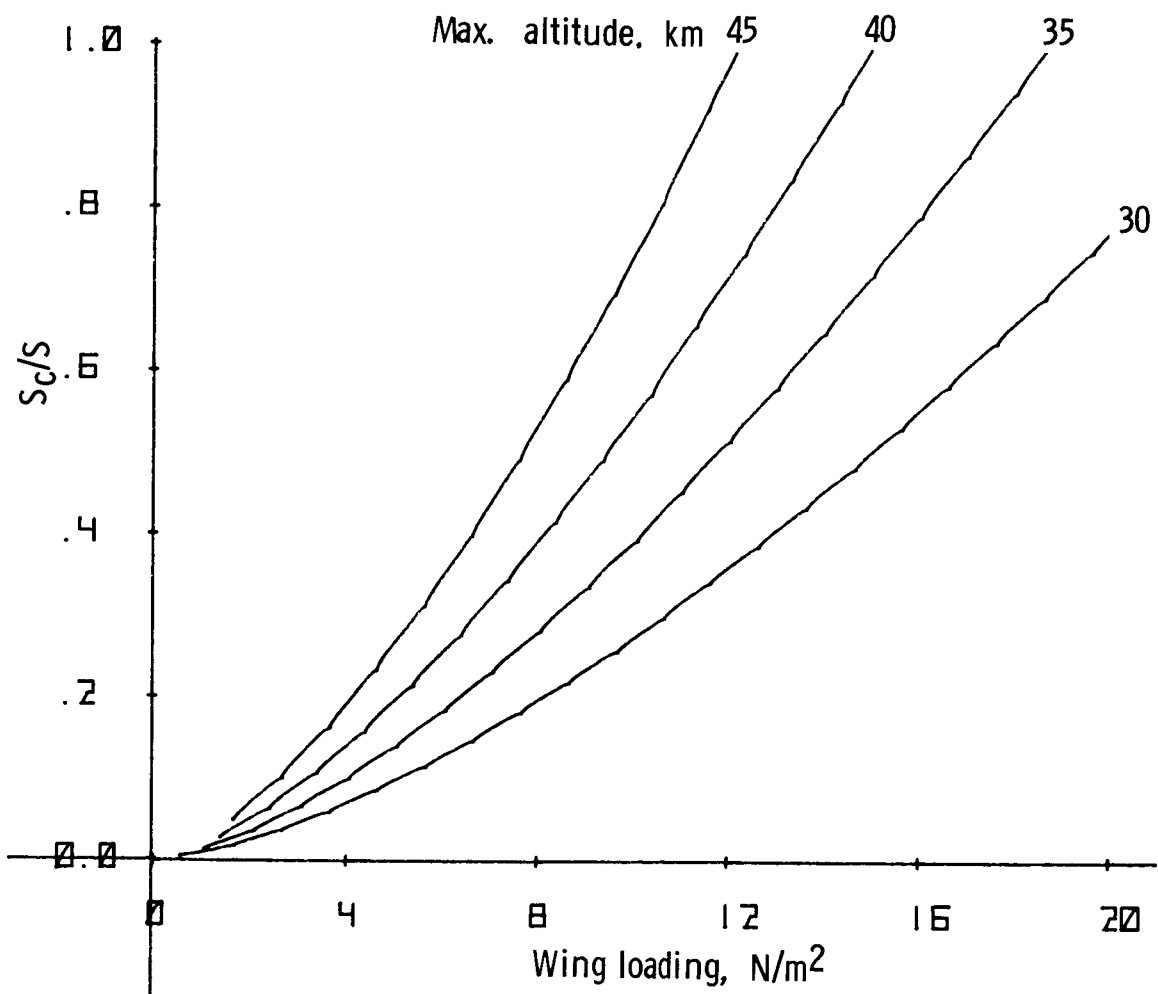
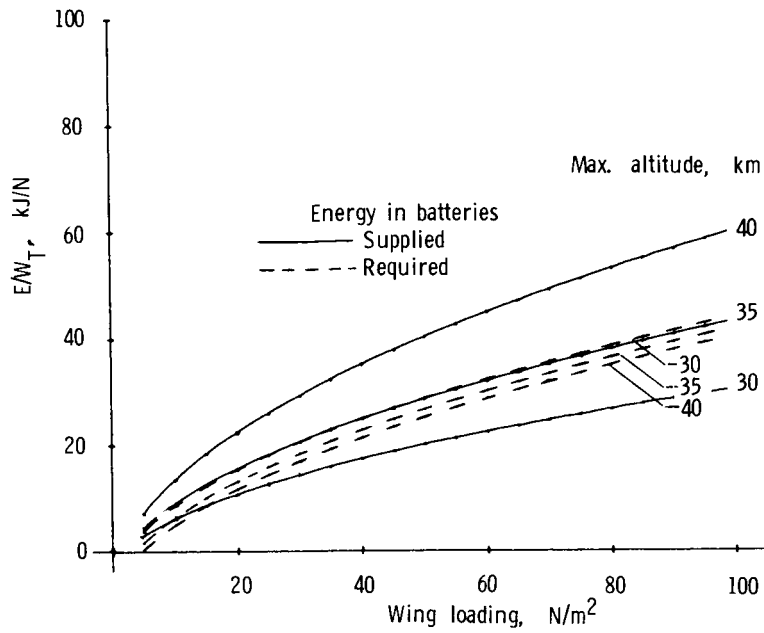
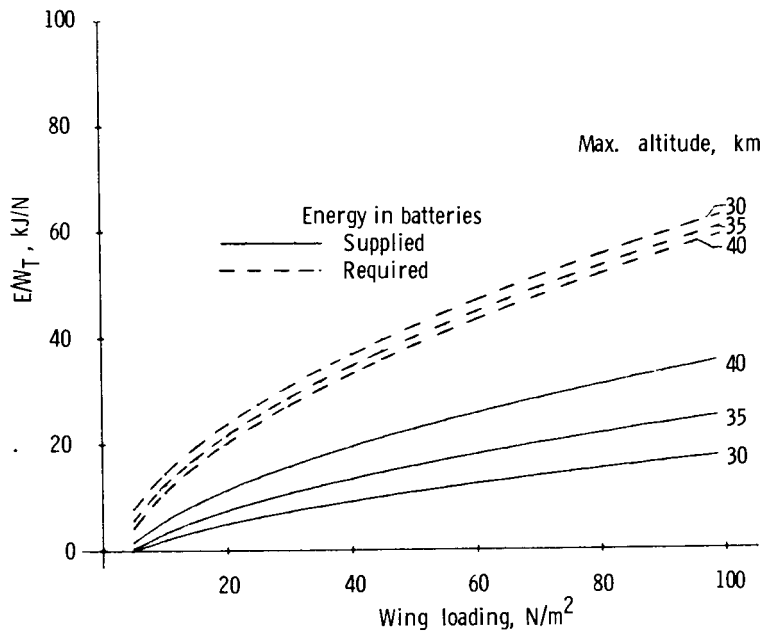


Figure 13.- Ratio of solar-cell area to wing area as function of wing loading for climb and descend mode of operation. Base altitude = 30 km; $C_L = 1.5$; $C_D = 0.07581$. Absolute ceiling 10 km above maximum altitude. Solar-cell area shown is that required to supply motor power in climb and is, therefore, independent of t_{night} .

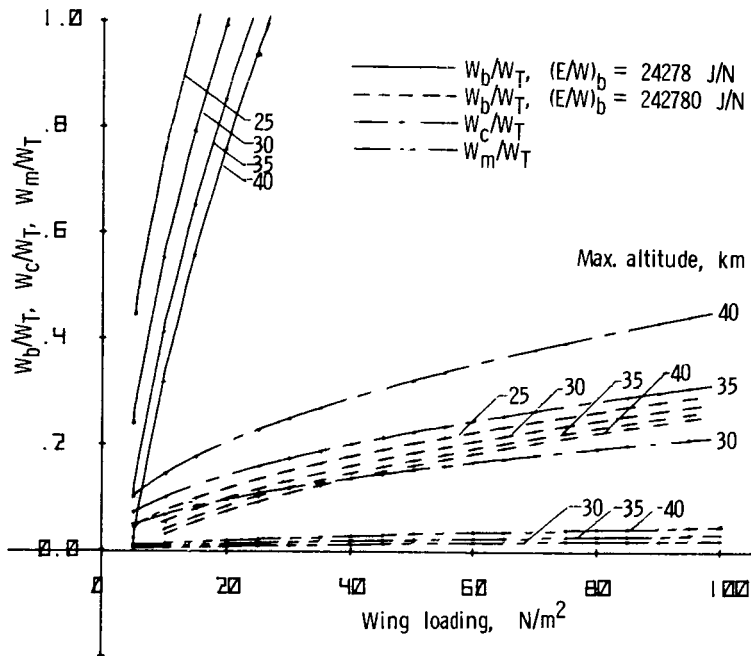


(a) $t_{\text{night}} = 12 \text{ hr.}$

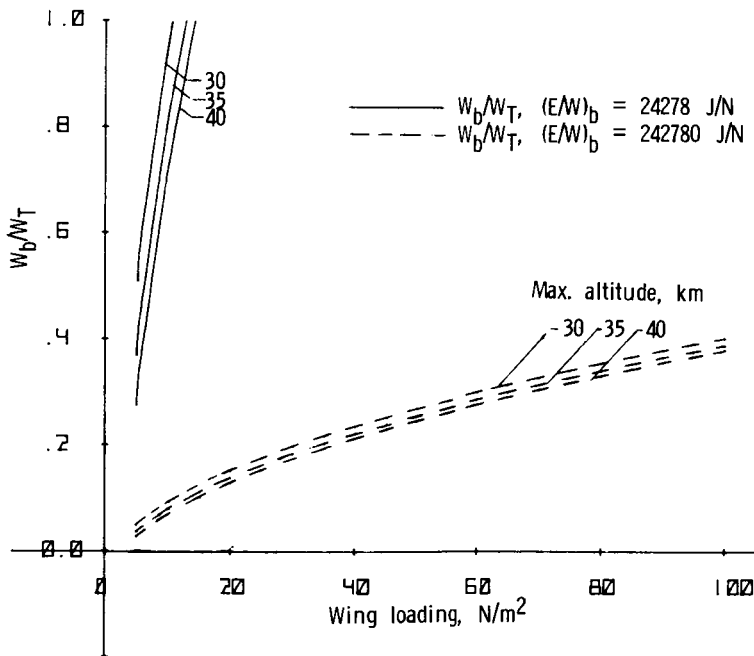


(b) $t_{\text{night}} = 16.3 \text{ hr.}$

Figure 14.- Energy per unit total weight supplied to batteries in segment ②-③ and required for level flight in segment ④-⑤ as function of wing loading for climb and descend mode of operation. Base altitude = 20 km; $C_L = 1.5$; $C_D = 0.04046$. Absolute ceiling 5 km above maximum altitude.

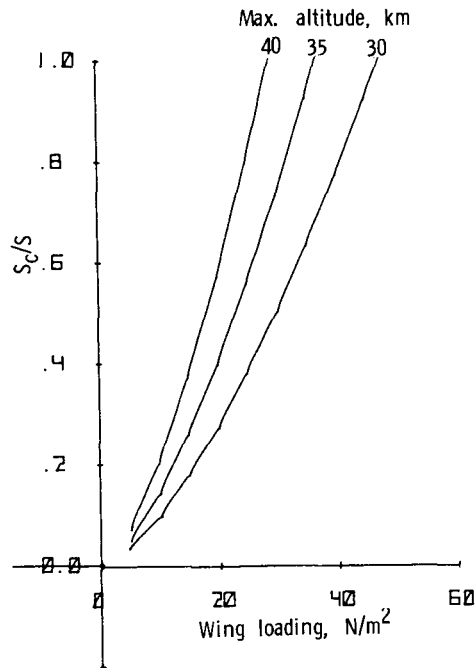


(a) $t_{\text{night}} = 12 \text{ hr.}$

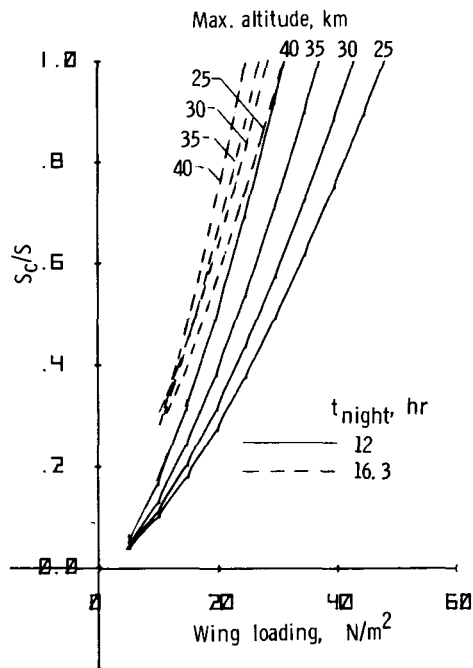


(b) $t_{\text{night}} = 16.3 \text{ hr.}$

Figure 15.- Ratios of weights of motor, solar cells, and batteries to total weight as functions of wing loading for climb and descend mode of operation. Base altitude = 20 km; $C_L = 1.5$; $C_D = 0.04046$. Absolute ceiling 5 km above maximum altitude. Motor weight and solar-cell weight are independent of t_{night} .



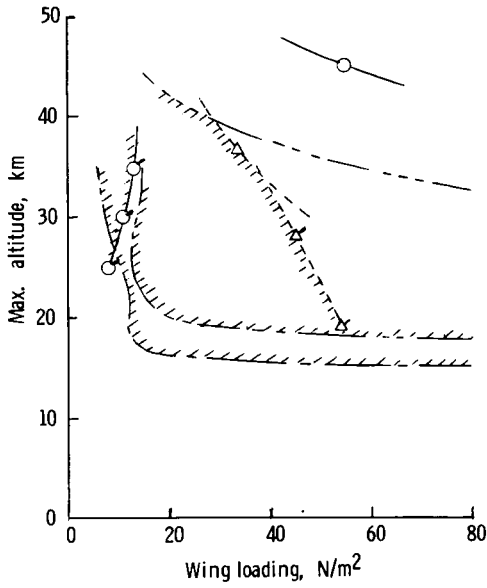
(a) Solar-cell area for climb (independent of t_{night}).



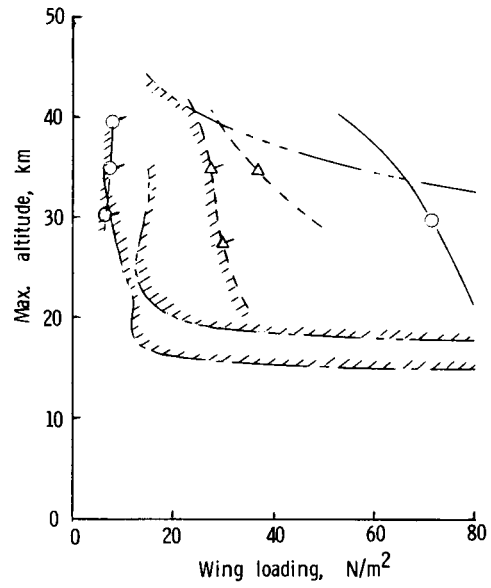
(b) Solar-cell area to charge batteries for night flight.

Figure 16.- Ratio of solar-cell area to wing area as function of wing loading for climb and descend mode of operation. Base altitude = 20 km; $C_L = 1.5$; $C_D = 0.04046$. Absolute ceiling 5 km above maximum altitude.

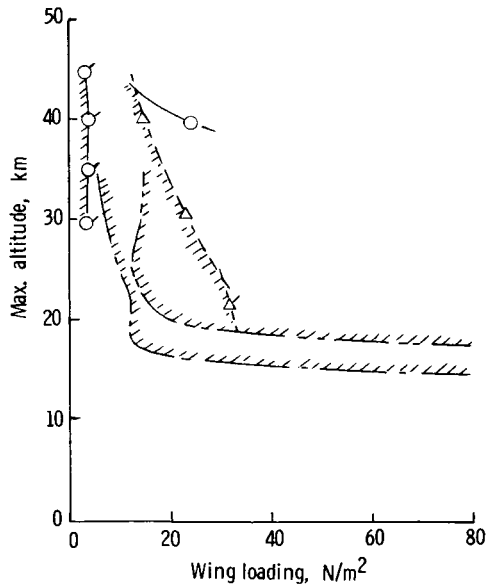
- $\Sigma W = 1, (E/W)_c = 242\,780 \text{ J/N}$
- $\Sigma W = 1, (E/W)_d = 24\,278 \text{ J/N}$
- - - $S_c/S = 1$, solar-cell area for climb
- - - $S_c/S = 1$, solar-cell area for charging batteries
- — — Winds (summer)
- — — Winds (winter)
- - - $M = 0.3$



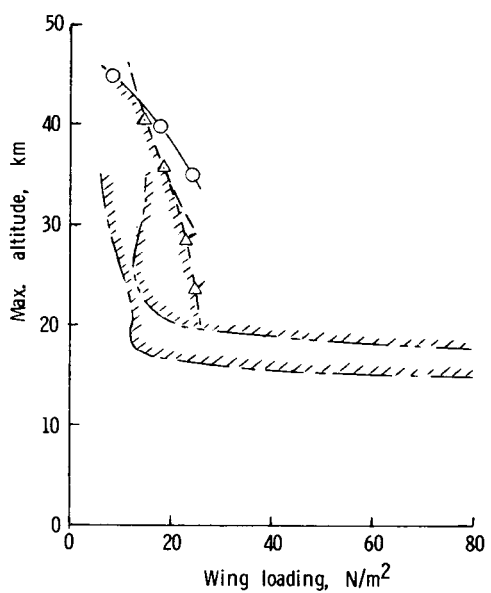
(a) $C_D = 0.04046$; $t_{\text{night}} = 12 \text{ hr.}$



(b) $C_D = 0.04046$; $t_{\text{night}} = 16.3 \text{ hr.}$



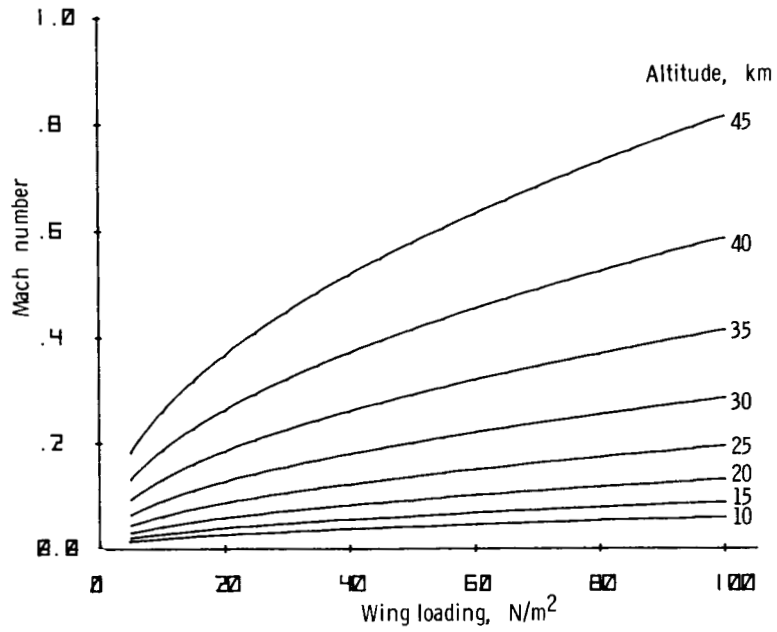
(c) $C_D = 0.07581$; $t_{\text{night}} = 12 \text{ hr.}$



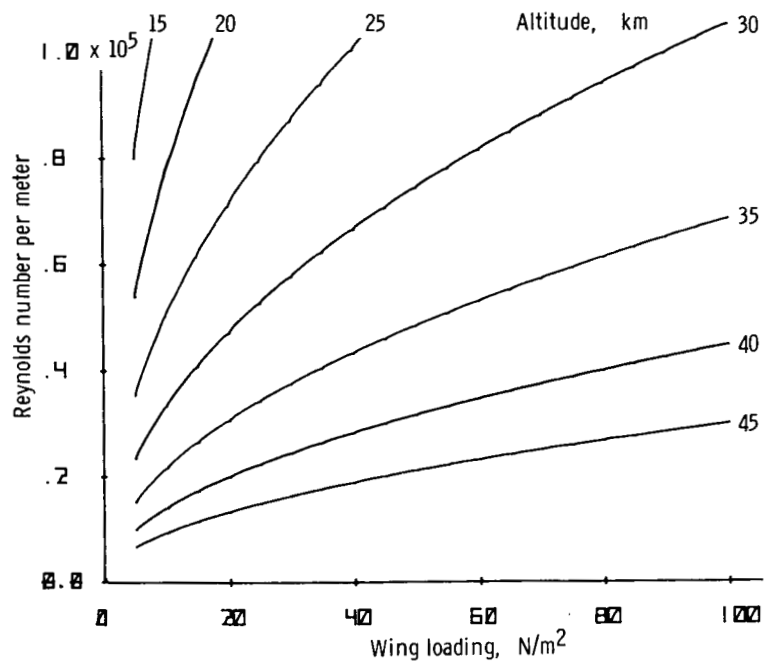
(d) $C_D = 0.07581$; $t_{\text{night}} = 16.3 \text{ hr.}$

Figure 17.- Regions of feasible operation in climb and descend mode of operation.

$C_L = 1.5$; Base altitude = 20 km.

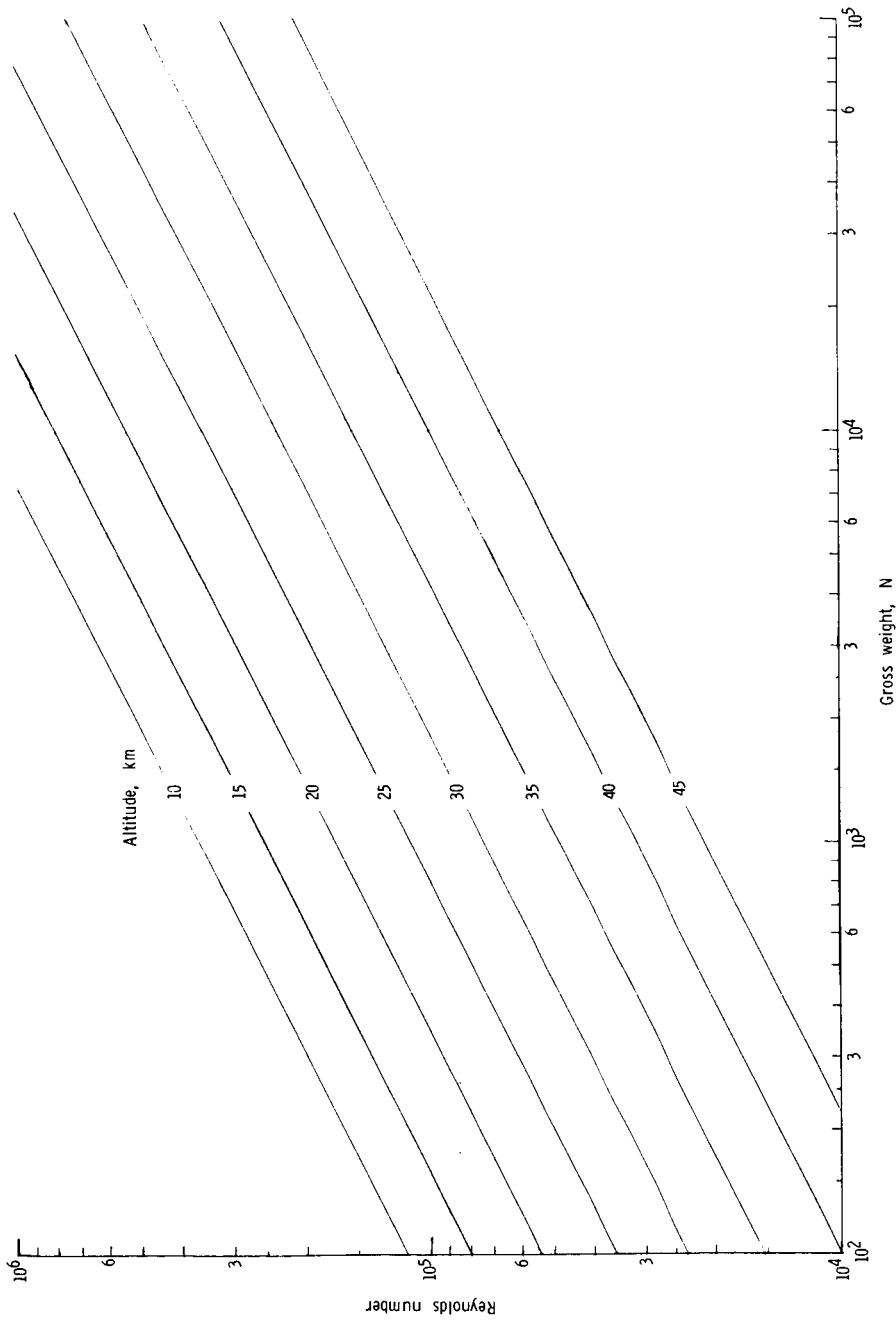


(a) Mach number.



(b) Reynolds number per meter.

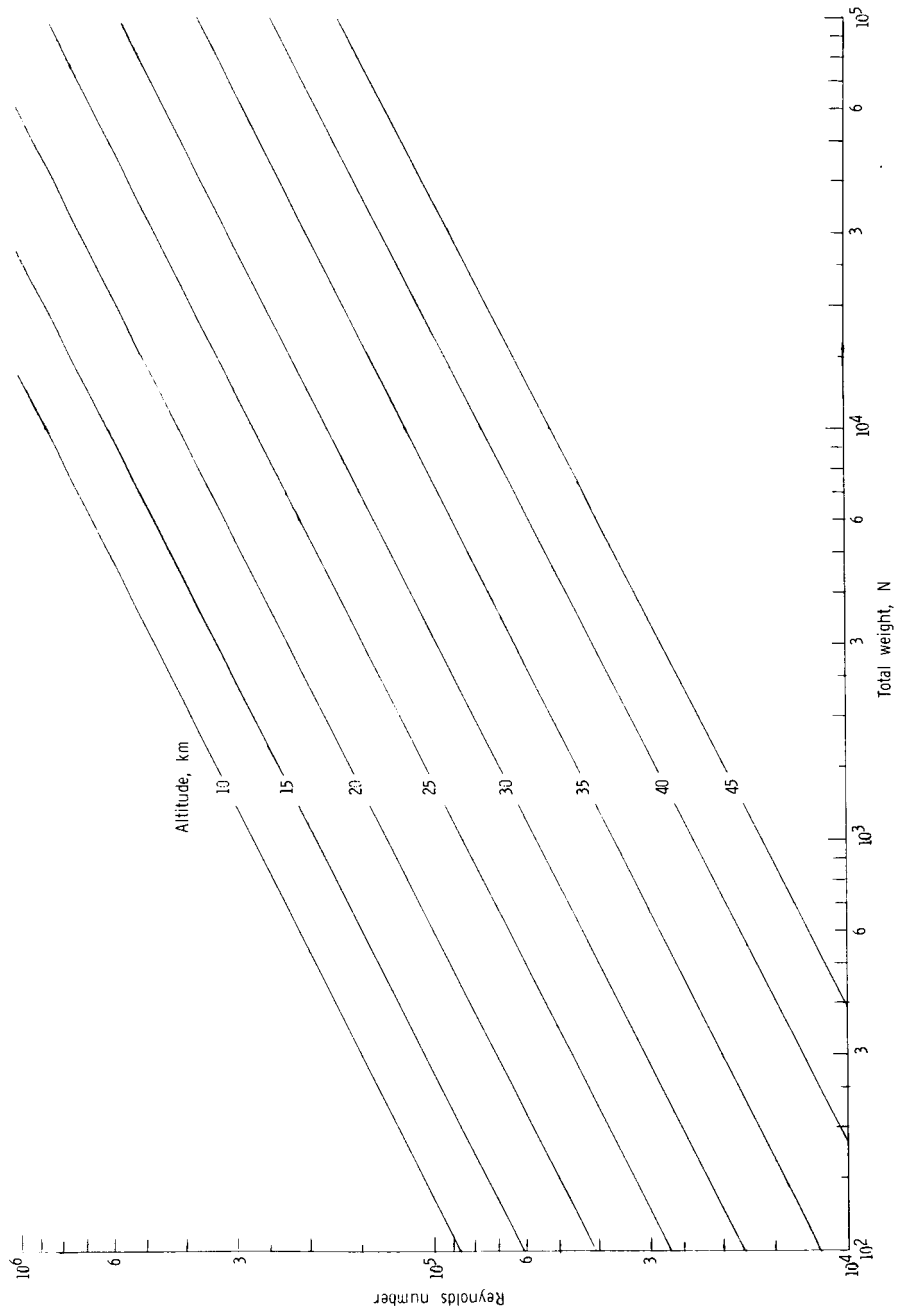
Figure 18.- Mach number and Reynolds number per meter as functions of wing loading for flight at various altitudes. $C_L = 1.5$.



(a) $C_{L,A} = 30$.

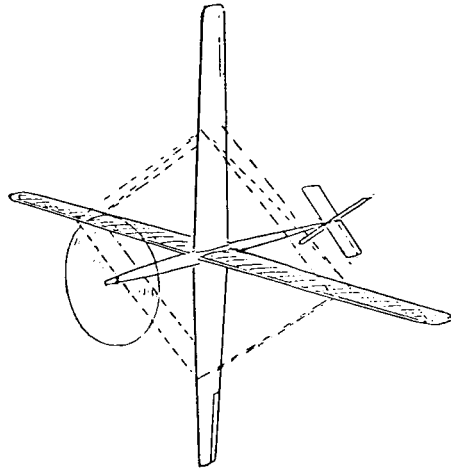
Figure 19. - Reynolds number based on mean chord as function of total weight for various values of altitude and for specified values of the product $C_{L,A}$. These results are calculated from the equation

$$\text{Reynolds number} = \frac{1}{\nu} \sqrt{\frac{2W_T \rho}{C_{L,A}}}$$

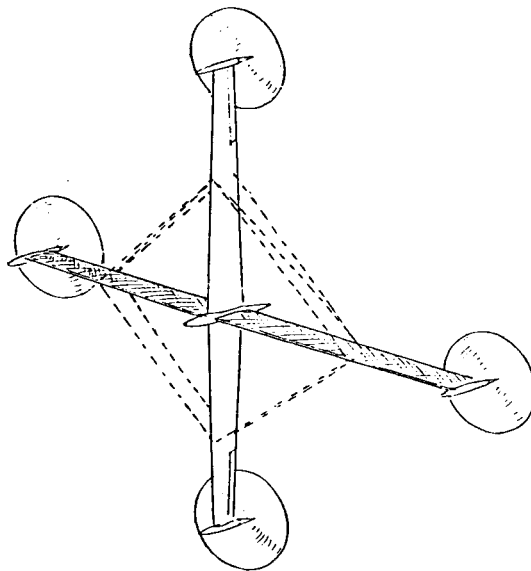


(b) $C_{L A} = 52.5$.

Figure 19.- Concluded.



(a) Solar-powered aircraft with cruciform wing. Cross-hatched areas indicate solar cells. Cruciform wing allows banking aircraft to maintain solar cells perpendicular to Sun line.



(b) Alternate arrangement of solar-powered aircraft with cruciform wing. Cross-hatched areas indicate solar cells. Stability and control in pitch and yaw are provided by actively controlled differential thrust of propulsion motors.

Figure 20.- Proposed configurations for solar-powered aircraft.

1. Report No. NASA TP-1675	2. Government Accession No.	3. Recipient's Catalog No.	
4. Title and Subtitle SOME DESIGN CONSIDERATIONS FOR SOLAR-POWERED AIRCRAFT		5. Report Date June 1980	6. Performing Organization Code
		8. Performing Organization Report No. L-13562	10. Work Unit No. 505-34-33-02
7. Author(s) William H. Phillips	9. Performing Organization Name and Address NASA Langley Research Center Hampton, VA 23665		11. Contract or Grant No.
12. Sponsoring Agency Name and Address National Aeronautics and Space Administration Washington, DC 20546			13. Type of Report and Period Covered Technical Paper
15. Supplementary Notes			
16. Abstract Analytical studies of performance and operating characteristics are presented for a solar-powered aircraft intended to remain aloft for long periods. The critical technologies which limit the performance are identified. By using the techniques presented, the effects of variation in the system parameters may be studied. A discussion of practical design considerations is included.			
17. Key Words (Suggested by Author(s)) Aircraft performance Solar-powered aircraft		18. Distribution Statement Subject Category 05	
19. Security Classif. (of this report) Unclassified	20. Security Classif. (of this page) Unclassified	21. No. of Pages 57	22. Price